Elsevier Editorial System(tm) for Ocean Engineering

Manuscript Draft

Manuscript Number: OE-D-17-00367R5

Title: Non-parametric Dynamic System Identification of Ships Using Multi-Output Gaussian Processes

Article Type: Full length article

Keywords: Dependent Gaussian processes; Dynamic System identification; Multi-output Gaussian processes; Non-Parametric Identification; Oceanic Vehicles

Corresponding Author: Mr. Wilmer Ariza Ramirez, Ph.D. Student, M.Eng. (AMT)

Corresponding Author's Institution: University of Tasmania

First Author: Wilmer Ariza Ramirez, Ph.D. Student, M.Eng. (AMT)

Order of Authors: Wilmer Ariza Ramirez, Ph.D. Student, M.Eng. (AMT); Zhi Leong, Dr.; Hung Nguyen, Dr.; Shantha Gamini Jayasinghe, Dr.

Abstract: A novel non-parametric system identification algorithm for a surface ship has been developed in this study with the aim of modelling ships dynamics with low quantity of data. The algorithm is based on multi-output Gaussian processes and its ability to model the dynamic system of a ship without losing the relationships between coupled outputs is explored. Data obtained from the simulation of a parametric model of a container ship is used for the training and validation of the multi-output Gaussian processes. The required methodology and metric to implement Gaussian processes for a 4 degrees of freedom (DoF) ship is also presented in this paper. Results show that multi-output Gaussian processes can be accurately applied for non-parametric dynamic system identification in ships with highly coupled DoF.

**Cover Letter**

Wilmer Ariza Ramirez
University of Tasmania
Maritime Way, Launceston,
Tasmania, Australia
Ph: 0404458032
Wilmer.arizaramirez@utas.edu.au

Dears Editor-in-Chief:

Atilla Incecik and Matthew Collette

I am pleased to submit an original research article entitled “Non-parametric Dynamic System Identification of Ships Using Multi-Output Gaussian Processes” for consideration for publication in the journal of Ocean Engineering.

In this manuscript, we propose a new algorithm for ship system identification by the application of multi-output Gaussian processes and its application to a container ship.

We believe that this manuscript is appropriate for publication by Ocean engineering because it covers a direct application of naval engineering and brings a tool for the application of nonlinear model predictive control.

This manuscript has not been published and is not under consideration for publication elsewhere. We have no conflicts of interest to disclose.

Thank you for your consideration!

Sincerely,

Wilmer Ariza Ramirez
PhD student
Australian Maritime College
University of Tasmania

**Highlights:**

- A methodology for the application of multi-output Gaussian processes for dynamic system identification of ships has been developed
- Qualities and defects of multi-output Gaussian processes based dynamic system identification are presented
- Study of the viability of Ship dynamic system identification with Multi-output Gaussian processes was executed to show the methodology and applicability

***Detailed Response to Reviewers**

**Response to reviewer's comments on the manuscript titled**
**'Non-parametric Dynamic System Identification of Ships Using Multi-Output Gaussian Processes'**

We would like to thank the editor for arranging a review for the manuscript and reviewers for spending their time to review the paper and providing valuable comments that helped improve the paper. All the comments are taken into serious consideration and suggested changes are incorporated in the revised manuscript. The following table lists our responses, corrections made, and locations of the changes made in the revised manuscript. Changes are highlighted in the revised manuscript.

Authors' responses to **Reviewer 5 comments**

| Comment Number | Comment | Changes | Location of the change | Authors' Comment |
|---|---|---|---|---|
| **1** | have read through paper and noticed that response to reviewer's comments and revised manuscript are not consistent. The promised changes have not been put into manuscript. | | | We apologize for this inconvenient, at the conversion of the file the changes were under review and we didn't notice that they didn't were accepted generating that the changes do not appear in the manuscript.<br><br>The change had been marked in yellow in the manuscript. |
| **2** | Comment 4: The notation is still ambigous. Why are you writting a matrix as an argument to function f?<br><br>"Page 10, line 191: This is strange notation for input vectors. If you insist in using it, add a reference to a published paper, not software, where this kind of notation is used for multi-input multi-output identification." | In the case of a four DoF ship, the system can be defined as a function $f$ that depends on a vector formed by the respective regressors of each output and the regressors of the command signals of propeller and rudder such as.<br>$\mathbf{y} = f\left(\mathbf{y}_{(k-1:n)}, \mathbf{u}_{RPM\,(k-1:n)}, \mathbf{u}_{rudder\,(k-1:n)}\right)$ | **Page 10 line 188-196** | We opted for a clearer and general notation in vector form. |

| | | | | |
|---|---|---|---|---|
| **3** | Comment 6: ... for each input. --> ... for each output. Apply this correction in two cases.<br><br>"Page 14, line 281: strange notation for multi-output system and not coherent with page 10, line 191.<br><br>Page 14, line 284: again strange notation and, moreover, the direct influence of input u(k) to output, which is not common for physical systems." | "The first system (RNN1) was a recurrent neural network system and it has a similar architecture to the Multi-output GPs $f\left[\mathbf{y}_{(k-1)}, \mathbf{u}_{RPM\,(k-1:2)}, \mathbf{u}_{rudder\,(k-1:2)}\right]$ for each output. The second NN system (NN2) use a common NARX identification methodology and used the last four delayed outputs of the system and the last delayed input commands $f\left[\mathbf{y}_{(k-1:4)}, \mathbf{u}_{\mathbf{1}(k-1:2)}, \mathbf{u}_{2(k-1:2)}\right]$ for each output." | **Page 14, line 281-284** | We have corrected it as suggested. |
| **4** | Comment 10: What does not encompass the entire operating region? Train data does. Expand the sentence.<br><br>"Page 17, Fig7abcd: Discuss the increasing variance with time! What are the good and bad consequences of the increasing variance? The variance is increasing because you predict in the non-identified region. This tells you that training signal is poor and does not encompass the entire operating region, so you need to justify the use of the selected training signal. Have you considered swapping or changing training and test signals?" | "The variance in our validation results increase as the data used for validation drift away from the trained operational region. This was done with the objective to test the capability of GPs to predict outside the trained operational region." | **Page 16, line 328** | We had added the discussion as suggested. We had tested other test signals and each one gives a similar results of increase in the validation variance. We theorizes that the normalization of the outputs produce a multiplication of variance between outputs if they had the same levels. However, the learning without this normalization show to be unsuccessful. |

# Non-parametric Dynamic System Identification of Ships Using Multi-Output Gaussian Processes

Wilmer Ariza Ramirez*[1], Zhi Quan Leong[1], Hung Nguyen[1], Shantha Gamini Jayasinghe[1]

[1]Australian Maritime College, University of Tasmania, Newnham TAS 7248, Australia
Wilmer.ArizaRamirez@utas.edu.au (* Corresponding author), Z.Leong@amc.edu.au, H.D.Nguyen@utas.edu.au, shanthaj@utas.edu.au

**Abstract**

A novel application of non-parametric system identification algorithm for a surface ship has been employ on this study with the aim of modelling ships dynamics with low quantity of data. The algorithm is based on multi-output Gaussian processes and its ability to model the dynamic system of a ship without losing the relationships between coupled outputs is explored. Data obtained from the simulation of a parametric model of a container ship is used for the training and validation of the multi-output Gaussian processes. The required methodology and metric to implement Gaussian processes for a 4 degrees of freedom (DoF) ship is also presented in this paper. Results show that multi-output Gaussian processes can be accurately applied for non-parametric dynamic system identification in ships with highly coupled DoF.

**Keywords**

Dependent Gaussian processes; Dynamic System identification; Multi-output Gaussian processes; Non-Parametric Identification; Oceanic Vehicles

## Introduction

Dynamic modelling of oceanic vehicles including surface ships, semisubmersibles/ submersible platforms, and unmanned underwater vehicles is an active research field due to the application importance of these vessels such as goods transport, oil and gas exploration (Olsgard and Gray, 1995), underwater survey, and fishery. The common approach to modelling such vehicles is the use of Newtonian-Lagrangian mathematical models which are usually predefined. However, the presence of unaccounted dynamics caused by parametric and non-parametric uncertainties in a predefined model can increase the error between the predicted output and the real output. The cause of these uncertainties is commonly attributed to ocean currents, waves, wind, and hydrodynamic interaction with nearby structures. Since oceanic vehicles operate in dynamically changing environments performance of traditional controllers such as PID, LQR, and backstepping controllers (Fossen, 2011; Pettersen and Nijmeijer, 2001) degrade over time of operation as they require an initial offline design, calibration and are directly dependent on the predefined system parameters. An optional approach to predefined mathematical modelling is the use of non-parametric system identification (SI) methods. In this context, the application of modern machine learning algorithms that are capable of producing evolutionary adaptability to the environment has been identified as a promising approach for SI (Ljung, 1999). The present study focuses on its application for the identification of surface ship dynamics.

There are multiple mathematical models for the representation of ships dynamics. Some models are 3 DoF models where the surge, sway and yaw are represented by linear and nonlinear equations (Abkowitz, 1964; Norrbin, 1971). Other more

advanced models such as (Son and Nomoto, 1982) used a 4 DoF nonlinear model for ships including the rolling effect. The dynamic modelling of ship is a prerequisite for the design of its autopilot, navigation, steering control, and damage identification systems. The exactitude of the model can lead to the reduction of fuel consumption (Källström et al., 1979) by the correct tuning of an autopilot, better vehicle stability, and less stress over the vehicle structure (Fossen, 1994) and the possibility of advanced algorithms such as automatic ship berthing (Ahmed and Hasegawa, 2013).

Dynamic mathematical models are usually obtained by the application of Newtonian and Lagrangian mechanics, which lead to a complex system of coupled equations defined by a series of parameters. The parameters are the representation of added masses, hydrodynamics damping constants, and constants related directly with control forces such as propellers and rudders. Over the years, multiple methods have been developed to determine the hydrodynamic parameters of ships, e.g. empirical formulas, captive model test, computational fluid dynamics (CFD) calculation and parameter estimation based in SI. The most recognized and accepted method is captive model test with planar motion mechanics (Bishop and Parkinson, 1970). This method requires the use of sophisticate facilities such as towing tanks, rotating arms and planar motion mechanism to produce the required ship manoeuvres that allow the parameters to be identified. These manoeuvres can also be replicated virtually via CFD which can be a more affordable option (Stern et al., 2011). However, as the accuracy of CFD is highly dependent on the numerical settings and requires validation, physical experiments are still preferred over computational solutions.

Parameter estimation based in SI methodologies offer a practical way to identify the hydrodynamic parameters of a ship model or a complete model. The data source for

SI can be free-running model tests or full-scales trials of existing ships. SI can be categorized in two groups, parametric and non-parametric identification. Parametric identification is based on the use of numerical methods to obtain the hydrodynamics parameters of proposed mathematical models with unknown parameters. Alternatively, non-parametric identification is based on the use of single or multiple kernel functions to create a non-physics related mathematical model which is tuned by a learning procedure that uses data obtained from the original system.

Methods like Extended Kalman Filter (Åström and Källström, 1976; Brinati and Neto, 1975), Unscented Kalman Filter(Zhou and Blanke, 1987), Estimation-Before-Modelling (Yoon and Rhee, 2003), and Backstepping (Casado et al., 2007) are the most popular numerical methods for coefficient estimation. However, these methods can suffer from linearization and convergence errors. Therefore, more advanced SI methods from machine learning, e.g. neural networks (Haddara and Wang, 1999), and support vector machines (Luo and Zou, 2009) had found their space in parametric ship SI with the use of specific structures (NN) or specific selection of kernel functions(SVM), these specific structure allow the techniques to calculate some coefficients. The principal disadvantage of parametric system identification is the need of controlled test with low external perturbations and specific procedures to reduce the interference and nonlinearities between degrees of freedom.

In contrast to the parametric SI, non-parametric SI has the capacity to learn a complete model without prior knowledge of the system structure. This learning procedure leads to a simpler model with fewer parameters. Non-parametric SI brings the possibility of incorporating online learning giving the ability to improve the adaptability of the model. The capability to adapt to change is very important for application of evolutionary control techniques and damage identification. The most

recognized method of non-parametric identification for ships is recursive neural network (RNN). RNN differs over standard neural networks in the aspect that the structure of the network is organized hierarchically applying the same set of weights recursively over the structure, to produce a scalar prediction on it. (Irsoy and Cardie, 2014). This method has been used with success to identify complex ship designs like catamarans with the final purpose of offline simulation of ship behaviours (Moreira and Soares, 2012). Wang et al. (2015) presented a modified version of SVMs to capture the full coupled system in four degrees of a ship following a similar methodology to RNNs. The difference between the SVM and the neural network methods is that the SMV is less prone to overfitting, thus can reach a global optimum and require less memory. Wang's proposed a white, grey and black box system, the black box is the result of the mathematical analysis of the grey black box that leads them to recognize an applicable kernel. The drawback of neural networks and SVM machine learning methods is the lack of confident measures, and thus, an error in the prediction cannot be corrected.

Depending on the budget and availability of infrastructure and time, the parametric or non-parametric model characterization can be chosen for a given system. In the case of new designs with low complexity, the parametric identification can be carried out without inconvenience as scale model can be produced and computational CAD files are available. However, for old oceanic vehicles that require fitting of new technology, vehicles that require operation in evolving environments, and vehicles with complex designs the use of non-parametric methods can be more practical.

Nevertheless, not all possible methods of machine learning had found their way to dynamic SI of ships. If a neural network is used to generate a non-parametric model with the inclusion of the variance, the number of hidden units ideally has to be taken

to infinity, in which case it turns that a neural network with infinite hidden layers is equivalent to another machine learning method known as Gaussian Processes (Neal, 2012). GPs is a well-established method in fields such as geostatistics, where the GPs method is renamed ‘kriging’ (Kbiob, 1951). In GPs based SI the model is built over input-output data and a covariance function is used to characterise the ship behaviour. The advantage of GPs is their ability to work with small quantities of data and noisy data, and the predicted results consist of a mean and variance value. The variance of a future prediction can be used for other purposes as well such as control and model based fault detection since it contains a measure of confidence. (Kocijan et al., 2005) and (Ažman and Kocijan, 2011) described the application of GPs for the identification of nonlinear dynamics system and provided examples over simple input and single outputs systems. The standard technique of modelling multi-output systems as a combination of single output GPs has the disadvantage of not modelling the coupling relationships among the outputs of a system as a ship. A ship is a system with highly related outputs where the absence of the relation between outputs can carry to error in prediction.

In the present study, non-parametric dynamic SI for ships is proposed with the use of multi-output GPs, NARX structure and gradient descent optimization. The output from the algorithm will be a predictive value and a measure of confidence of the predictive value. Multi-output GPs is a special case of GPs with the capability to model the nonlinear behaviour and coupling among outputs of a multi-output system. Ships are ideal candidates for the use of multi-output GPs owing to their dynamic system with highly coupled outputs, i.e. the ship’s motion in 4 DoF. The present implementation was made over data obtained from a non-conventional zig-zag test with variable frequency of a 4 DoF simulated container ship. Multiple sample times

and data length were tested to find the best metric that can describe a ship. In addition to the algorithm development, another immediate objective of the study is the demonstration of the viability of GPs in modelling ships.

**Nonlinear Dynamic Ship Model**

(Son and Nomoto, 1982) proposed a 4 DoF (surge, sway, yaw and pitch) mathematical nonlinear model for ships including the contribution from hydrodynamics added masses. In respect to a body fixed frame (Fig. 1) the mathematical model can be expressed as:

$$\begin{aligned}
&\left(m+m_x\right)\dot{u}-\left(m+m_y\right)vr = X\\
&\left(m+m_y\right)v+\left(m+m_x\right)ur+m_y\alpha_y\dot{r}-m_y l_y\dot{p} = Y\\
&\left(I_x+J_x\right)\dot{p}-m_y l_y\dot{v}-m_x l_x ur = K-W\overline{GM_T}\phi\\
&\left(I_z+J_z\right)\dot{r}+m_y\alpha_y\dot{v} = N-x_G Y
\end{aligned} \tag{1}$$

Fig. 1 here

where the added mass in x-axis and y-axis are represented by $m_x$, $m_y$ and the added moment of inertia about x-axis and y-axis are represented by $J_x$ and $J_y$. The centre of added mass is denoted by the vector $\left(\alpha_x,\alpha_y,\alpha_z\right)$, while the added mass centre for $m_x$ and $m_y$ is denoted by the z-coordinates of $l_x$ and $l_y$. The vector $[X,Y,K,N]$ expresses the forces over the vehicle and can be defined as:

$$
\begin{aligned}
X &= X(u) + (1-t)T + X_{vr}vr + X_{vv}v^2 + X_{rr}r^2 \\
&\quad + X_{\phi\phi}\phi^2 + X_{\delta}\sin(\delta) + c_{RX}F_N \sin\delta \\
\\
Y &= Y_v v + Y_r r + Y_\phi \phi + Y_p p + Y_{vvv}v^3 + Y_{rrr}r^3 \\
&\quad + Y_{vvr}v^2 r + Y_{vrr}vr^2 + Y_{vv\phi}v^2\phi + Y_{v\phi\phi}v\phi^2 \\
&\quad + Y_{rr\phi}r^2\phi + Y_{r\phi\phi}r\phi^2 + Y_{\delta}\cos(\delta) \\
&\quad - (1+a_H)\, z_R F_N \cos\delta \\
\\
K &= K_v v + K_r r + K_\phi \phi + K_p p + K_{vvv}v^3 + K_{rrr}r^3 \\
&\quad + K_{vvr}v^2 r + K_{vrr}vr^2 + K_{vv\phi}v^2\phi + K_{v\phi\phi}v\phi^2 \\
&\quad + K_{rr\phi}r^2\phi + K_{r\phi\phi}r\phi^2 + K_{\delta}\cos(\delta) \\
&\quad + (1+a_H)\, F_N \cos\delta \\
\\
N &= N_v v + N_r r + N_\phi \phi + N_p p + N_{vvv}v^3 + N_{rrr}r^3 \\
&\quad + N_{vvr}v^2 r + N_{vrr}vr^2 + N_{vv\phi}v^2\phi + N_{v\phi\phi}v\phi^2 \\
&\quad + N_{rr\phi}r^2\phi + N_{r\phi\phi}r\phi^2 + N_{\delta}\cos(\delta) \\
&\quad + (x_R + a_H x_H)\, z_R F_N \cos\delta
\end{aligned}
\tag{2}
$$

where:

$X(u)$ = function dependent on the velocity $X_{|u|u}|u|u$

$\delta$ = rudder angle

$F_N$ =rudder force

$X_{vr}X_{vv},...N_{r\phi\phi}$ =model parameters

As can be seen, the mathematical model is defined by more than 50 parameters including parameters from the actuation surfaces. An example of the hydrodynamic parameters and its application can be found in Fossen (1994).

**Dynamic Identification with Multi-output GPs**

The design of the algorithm for multi-output SI with GPs is based on the previous work of Kocijan (2016). The dynamic identification problem can be defined as the search for relation between a vector formed by delayed samples from the inputs $u(k)$ and outputs $y(k-1)$ and the future output values. The relationship can be expressed by the equation:

$$\mathbf{y}(k+1) = f\left(\mathbf{z}(k), \boldsymbol{\Theta}\right) + v(k) \tag{3}$$

where $f\left(\mathbf{z}(k), \boldsymbol{\Theta}\right)$ is a function that maps the sample data vector $\mathbf{z}(k)$ that contains the vector $[\mathbf{u}(k-1), \mathbf{y}(k-1)]$ to the output space based on the hyperparameters $\boldsymbol{\Theta}$. $\mathbf{v}(k)$ accounts for the noise and error in the prediction of output $\mathbf{y}(k)$. In the case of dynamic SI, the discrete time variable $(k)$ is presented as an embedded element in the regression process as it is accounted in the delayed samples.

A requirement for dynamic SI of nonlinear systems is the selection of a nonlinear model structure as nonlinear autoregressive model with exogenous input (NARX), nonlinear autoregressive (NAR), nonlinear output-error (NOE), nonlinear finite-impulse response (NFIR), etc. From all the possible structures, the simpler and most popular structure to implement is NARX as its predictions are based on previous measurements of the input signals and output signals and require a more simplified optimization scheme. In the case of a ship, NARX is the most practical configuration since the measuring points are restricted to the available sensors. Fig. 2 shows the NARX configuration for Dynamic GPs for a simple case of one-input one-output system.

Fig. 2 here

In the case of a single-input single-output structure NARX for a GPs, the inputs signals are not considered separately as they are grouped into a single vector of dimension $n$ that derives to an output of single dimension. In the case of a four DoF ship, the system can be defined a function $f$ who depends of a vector formed by the respective regressors of each output and the regressors of the command signals of propeller and rudder such as.

$$\mathbf{y} = f\left(\mathbf{y}_{(k-1:n)}, \mathbf{u}_{RPM\,(k-1:n)}, \mathbf{u}_{rudder\,(k-1:n)}\right)$$

If a Newton-Lagrange mathematical model had been used, our system will have two-input signals, four-output system signals. (Fig. 3) presents the graphical representation of the NARX architecture used with multi-output GPs with four vector of dimension R3.

Fig. 3 Here

**Multi-output GPs**

The previous sections outline Eq.(1) and Eq.(2) which show the level of coupling between the Newton-Lagrange equations of a ship. The nonlinearity and coupling between outputs are better represented by a multi-output GPs. multi-output GPs presented here is based on the work of Alvarez and Lawrence (2009). multi-output GPs are founded in the regression of data by the convolution of white noise process with a smoothing function(Higdon, 2002). This was later introduced by Boyle and Frean (2004) to the machine learning community by assuming multiple latent process defined over a space $\Re^q$. The dependency between two outputs is modelled with a common latent process and their independency with a latent function who does not interact with other outputs. If a set of functions $\left\{f_q(\mathbf{x})\right\}_{q=1}^{Q}$ is considered,

where $Q$ is the Output Dimension for a $N$ number of data points, where each function is expressed as the convolution between a smoothing kernel $\{k_q(\mathbf{x})\}_{q=1}^{Q}$ and a latent function $\mathbf{u}(z)$ ,

$$f_q(x) = \int_{-\infty}^{\infty} k_q(\mathbf{x}-\mathbf{z})u(\mathbf{z})d\mathbf{z} \tag{4}$$

This equation can be generalized for more than one latent function $\{u_r(\mathbf{x})\}_{r=1}^{R}$ and include a corruption function (noise) independent to each of the outputs $w_q(\mathbf{x})$, to obtain

$$\begin{aligned}\mathbf{y}_q(\mathbf{x}) &= f_q(\mathbf{x}) + w_q(\mathbf{x}) \\ \mathbf{y}_q(\mathbf{x}) &= \sum_{r=1}^{R}\int_{-\infty}^{\infty} k_{qr}(\mathbf{x}-\mathbf{z})u_r(\mathbf{z})d\mathbf{z} + w_q(\mathbf{x})\end{aligned} \tag{5}$$

The covariance between two different functions $y_q(x)$ and $y_s(x')$ is:

$$\begin{aligned}\operatorname{cov}\left[\mathbf{y}_q(\mathbf{x}),\mathbf{y}_s(\mathbf{x}')\right] &= \operatorname{cov}\left[f_q(\mathbf{x}),f_s(\mathbf{x}')\right] \\ &\quad + \operatorname{cov}\left[w_q(\mathbf{x}),w_s(\mathbf{x}')\right]\delta_{qs}\end{aligned} \tag{6}$$

where

$$\begin{aligned}\operatorname{cov}\left[f_q(\mathbf{x}),f_s(\mathbf{x}')\right] &= \sum_{r=1}^{R}\sum_{p=1}^{R}\int_{-\infty}^{\infty} k_{qr}(\mathbf{x}-\mathbf{z}) \\ &\quad \int_{-\infty}^{\infty} k_{sp}(\mathbf{x}'-\mathbf{z}')\operatorname{cov}\left[u_r(\mathbf{z}),u_p(\mathbf{z}')\right]d\mathbf{z}'d\mathbf{z}\end{aligned} \tag{7}$$

If it is assumed that $u_r(\mathbf{z})$ is an independent white noise $\operatorname{cov}\left[u_r(\mathbf{z}),u_p(\mathbf{z}')\right] = \sigma_{ur}^2\delta_{rp}\delta_{z,z'}$ ,

Equation (7) will become:

$$\operatorname{cov}\left[f_q(\mathbf{x}),f_s(\mathbf{x}')\right] = \sum_{r=1}^{R}\sigma_{ur}^2\int_{-\infty}^{\infty} k_{qr}(\mathbf{x}-\mathbf{z})k_{sp}(\mathbf{x}'-\mathbf{z}')d\mathbf{z} \tag{8}$$

The mean $\hat{\mathbf{y}}'$ with variance $\boldsymbol{\sigma}_{\hat{\mathbf{y}}'}$ of a predictive distribution at the point $\mathbf{x}'$ given the hyperparameters $\boldsymbol{\Theta}$ can be defined as

$$\hat{\mathbf{y}}' = k(\mathbf{x}', \mathbf{x})k(\mathbf{x}, \mathbf{x})^{-1}\mathbf{y} \tag{9}$$

and variance

$$\boldsymbol{\sigma}^2_{\hat{y}'} = k(\mathbf{x}', \mathbf{x}') - k(\mathbf{x}', \mathbf{x})^T k(\mathbf{x}, \mathbf{x})^{-1} k(\mathbf{x}', \mathbf{x}) \tag{10}$$

A complete explanation over the convolution process can be found in (Alvarez and Lawrence, 2009) and a complete implementation in Alvarez and Lawrence (2014).

**Learning Hyperparameters**

There are two principal methods for learning the hyperparameters $\Theta$, Bayesian model interference and marginal likelihood. Bayesian inference is based on the assumption that a prior data of the unknown function to be mapped is known. A posterior distribution over the function is refined by incorporation of observations. The marginal likelihood method is based on the aspect that some hyperparameters are going to be more noticeable. Over this base the posterior distribution of hyperparameters can be described with a unimodal narrow Gaussian distribution.

The learning of GPs hyperparameters $\Theta$ is commonly done by the maximization of the marginal likelihood. The marginal likelihood can be expressed as:

$$p\left(\mathbf{y}|\mathbf{x}, \boldsymbol{\Theta}\right) = \frac{1}{(2\pi)^{\frac{N}{2}}|\mathbf{K}|^{\frac{1}{2}}} e^{-\frac{1}{2}\mathbf{y}^T\mathbf{K}^{-1}\mathbf{y}} \tag{11}$$

where $\mathbf{K}$ is the covariance matrix, $N$ is the number of input learning data points and $y$ is a vector of learning output data of the form $\left[y_1; y_2; \cdots y_N\right]$. To reduce the

calculation complexity, it is preferred to use the logarithmical marginal likelihood that is obtained by the application of logarithmic properties to (11).

$$\mathcal{L}(\boldsymbol{\Theta}) = -\frac{1}{2}\log(|\mathbf{K}|) - \frac{1}{2}\mathbf{y}^T\mathbf{K}^{-1}\mathbf{y} - \frac{N}{2}\log(2\pi) \tag{12}$$

To find a solution for the maximization of log-likelihood multiples methods of optimization can be applied, like, particle swarm optimization, genetic algorithms, or gradient descent. For deterministic optimization methods, the computation of likelihood partial derivatives with respect to each hyperparameter is require. From (Williams and Rasmussen, 2006, p. 114) log-likelihood derivatives for each hyperparameter can be calculated by:

$$\frac{\partial\mathcal{L}(\boldsymbol{\Theta})}{\partial\boldsymbol{\Theta}_i} = -\frac{1}{2}trace\left(\mathbf{K}^{-1}\frac{\partial\mathbf{K}}{\partial\boldsymbol{\Theta}_i}\right) + \frac{1}{2}\mathbf{y}^T\mathbf{K}^{-1}\frac{\partial\mathbf{K}}{\partial\boldsymbol{\Theta}_i}\mathbf{K}^{-1} \tag{13}$$

Equation (12) gives us the learning process computational complexity, for each cycle the inverse of the covariance matrix of $\mathbf{K}$ has to be calculated. This calculation carries a complexity $\mathbf{O}(\mathbf{NM})^3$ where $N$ is the number of data points and $M$ is the number of outputs of the system. After learning, the complexity of predicting the value $\mathbf{y}(k+1)$ is $\mathbf{O}(\mathbf{NM})$ and to predict the mean value $\boldsymbol{\sigma}(k+1)$ is $\mathbf{O}(\mathbf{NM})^2$ .The higher training complexity $\mathbf{O}(\mathbf{NM})^3$ is the major disadvantage of using multi-output GPs. If the number of data increases the complexity of learning the hyperparameters increases in a cubic form. Methods such as genetic algorithms, differential equations, and particle swarm optimization can be applied to avoid the calculation of the marginal likelihood partial derivatives and thereby reduce the computational time.

## Experiment Setup and Results

### Experiment setup

The implementation of Son and Nomoto (1982) mathematical model of a container ship programmed in the Marine Systems Simulator (Fossen and Perez, 2004) was used to create the required databases. The container ship particulars can be found in Table 1. A simulation setup was developed in MATLAB/Simulink to emulate the behaviour of a container ship (Fig. 4). 1400 seconds were simulated where the inputs signals are constant shaft speed in RPM and a cosine signal with frequency change for rudder angle in radians (Fig. 5). The objective of not using a standard test as zigzag or turning circle is to test the ability of GPs for online learning. A sample data point was captured for each three steps over the input and outputs. A total of 1868 points were captured over four outputs and 934 point over two input signals. The data set was divided in two sets of points, the first set of points is used for the model learning, and the second set of points is used for learning validation. The Validation data is purposely chosen to be beyond the range of training data to test the ability of the method to predict beyond the training range. Two neural network nonlinear system identification models were also prepared. The first system (RNN1) was a recurrent neural network system and it has a similar architecture to the Multi-output GPs $f\left[\mathbf{y}_{(k-1)}, \mathbf{u}_{RPM\,(k-1:2)}, \mathbf{u}_{rudder\,(k-1:2)}\right]$ for each output. The second NN system (NN2) use a common NARX identification methodology and used the last four delayed outputs of the system and the last delayed input commands $f\left[\mathbf{y}_{(k-1:4)}, \mathbf{u}_{\mathbf{1}(k-1:2)}, \mathbf{u}_{2(k-1:2)}\right]$ for each output. The neural network systems use a Log-sigmoid transfer function, at different of GPs the training of NN was done by Levenberg-Marquardt backpropagation. Both neural network systems were trained, validated, and tested with the same data used for the multi-output GPs. The complete implementation code can be found at the GitHub Repository (FOOTNOTE 1).

Table 1 Particulars of Container Ship

| Parameter | Magnitude | |
|---|---|---|
| Length overall | 175 | m |
| Breadth | 25.4 | m |
| Max. Rudder Angle | 10 | deg. |
| Max. shaft velocity | 160 | Rpm |
| Displacement Volume | 21222 | $m^3$ |
| Rudder Area | 33.0376 | $m^2$ |
| Propeller diameter | 6.533 | m |

Fig. 4 Here

Fig. 5 Here

**Training and validation**

The software written by Alvarez and Lawrence (2014) was softly modified to accept the multidimensional input vectors and a script was written to implement the NARX structure. The convolution of two square exponential Gaussian processes and a white noise was chosen as kernel. The inputs of the GPs were defined as four inputs of dimension five of the form:

$$\begin{bmatrix} \dot{u}_k \\ v_k \\ r_k \\ p_k \end{bmatrix} = f\left(\mathbf{y}_{k-1}, \mathbf{u}_{RPM\,(k-1:2)}, \mathbf{u}_{rudder\,(k-1:2)}\right) \tag{14}$$

where $\mathbf{y}_{k-1}$ is the first regressor of the output vector $[\dot{u}_k, v_k, r_k, p_k]$.

The selection of the structure of regressors was determined via the examination of the mathematical model. Each output is affected by the past states of output and rudder force $F_N$ produced by the interaction of the rudder angle and the propeller RPM as both signals are required for the calculation of $F_N$. Under this assumption different structures were tested to verify the responsiveness to each regressor. The test showed that the container ship system is more responsive to regressors from the rudder angle and the propeller RPM.

The captured output vector was the derivative of surge speed, the speed in sway and the angular speeds of yaw and roll, $[\dot{u}, v, r, p]$. As can be seen in eq.(1) and eq.(2) the surge speed is not highly couple to the other system outputs, in our simulation capturing the surge speed and posterior simulation was not converging to the real output, in contrast the surge speed derivative shows coupling with other system outputs. The input signals and outputs were normalized between -1 and 1 to give all the inputs and outputs the same weight in the learning process.

For the training, the minimization of the negative logarithmical likelihood was used along with the scaled conjugate gradient with multiple start points to insure convergence. Fig. 6 shows the results of GPs training compared to the real system signals, and the error plots between the predicted and real systems. In all the graphs, a confidence band $2\sigma$ is plotted. The error for the surge derivative is less than 0.02 over the training data.

Fig. 6a Here

Fig. 6b Here

Fig. 6c Here

Fig. 6d Here

The validation data consisted of the real output from the training data with the system delay $(k-1)$ in vector form with the delayed commanded inputs. The segments of results from the validation with the second set of data are depicted in Fig. 7, the predicted output and confidence of $2\sigma$ band is portrayed in comparison to the original system. The low validation errors show a good system prediction for the sway speed and yaw speed. It can be notice that the simulation precision is lose by how far from the training data the step is. The variance in our validation results increase as the data used for validation drift away from the trained operational region.

This was done with the objective to test the capability of GPs to predict outside the trained operational region.

Fig. 7a Here

Fig. 7b Here

Fig. 7c Here

Fig. 7d Here

**Simulation**

A third step was implemented in the way of a naive simulation. Methods of control with non-parametric models require a number of step forward of prediction to be able to control a system. With the objective of testing the ability to predict a system from past data, a naive simulation was setup. At each step the output from the simulation is feedback to the simulation as the past input $y_i(k-1)$, the initial position and control signal of rudder and forward speed where used, the naive simulation covers training(0-700s) and validation data(701-1400s) acquired from the original simulation. Table 2 shows the root mean square error (RMSE), the predicted residual error sum of squares (PRESS) measurements for the simulation stage over the training and validation data, and the training time and step simulation time for each of the methodologies. The RMSE and PRESS value for the proposed GPs are smaller than the other systems. As evident in Fig. 8(a-c) NNARX system with the same architecture (marked as NarxNN) and data as in the multi output GPs has limitations in the capability to predict the system behaviour beyond the training range in all DoF. The more complex RNN system (RNN1) produces relatively good results, except in predicting the surge. This is evident Fig. 8 (a) where RNN1 results in large deviations

from the original system, especially after 1000s.The yaw output in Fig. 8 (c) shows a higher variance as results of higher association to the other outputs of the system and similitude to other training data this is because of normalization of the outputs in the training data. The difference in capability of prediction of the system is related to their internal functions and how they relate the training data. In comparison to NNRX and RNN, the multi-output GPs show similar performance than RNN outside the training horizon in all the DoF. This is evident in all the results shown in Fig. 8 with the close match to the system from the simulation, it can be established that the Gaussian model can be used for applications as control and failure detection as it can predict future system states with the added value of a confidence measure.

Table 2 Summary prediction quality measurements

| | **GPs** | **NarxNN** | **RNN1** |
|---|---|---|---|
| **RMSE** | 0.0091 | 0.0092 | 0.044 |
| **PRESS** | 0.2327 | 5.47 | 0.2382 |
| **Training time(s)** | 779 | 245 | 125 |
| **Step simulation time** | 0.0625 | 0.032 | 0.027 |

Fig. 8a Here

Fig. 8b Here

Fig. 8c Here

Fig. 8d Here

## Conclusion

The basic methodology for the use of multiple-output Gaussian distribution for the identification of ships dynamical models is presented in this paper. The methodology has been validated with the data obtained from a coupled dynamical system of a container ship. With the proposed Gaussian model, the large number of system parameters found in a typical ship model can be reduced to a smaller number of hyperparameters. A standard validation process of machine learning and prediction

over the complete data set of training and validation were executed to establish the model quality and robustness of the algorithm. The prediction of the full set of data based in a start value and feedback from the last prediction step show low error. As the results indicate, multi-output GPs has the ability to model complex dynamic system having highly coupled outputs and provide a measure of the confidence represented by the variance.

The use of other methods such as sparse multi-output GPs and the use of more powerful prediction techniques as Taylor series or Montecarlo method can take advantage of the variance to increase the horizon of cover manoeuvres and the prediction accuracy. Although the results obtained look encouraging, conclusion about the practical value of the method can only be obtained by comparison with other GPs methods and validation with real data from a ship or other oceanic vehicle.

## References


Abkowitz, M.A., 1964. Lectures on ship hydrodynamics--Steering and manoeuvrability.

Ahmed, Y.A., Hasegawa, K., 2013. Automatic ship berthing using artificial neural network trained by consistent teaching data using nonlinear programming method. Engineering Applications of Artificial Intelligence 26 (10), 2287-2304.

Alvarez, M., Lawrence, N., 2014. Multiple output Gaussian processes in MATLAB, Github, GitHub repository.

Alvarez, M., Lawrence, N.D., 2009. Sparse convolved Gaussian processes for multi-output regression, Advances in neural information processing systems, pp. 57-64.

Åström, K.J., Källström, C., 1976. Identification of ship steering dynamics. Automatica 12 (1), 9-22.

Ažman, K., Kocijan, J., 2011. Dynamical systems identification using Gaussian process models with incorporated local models. Engineering Applications of Artificial Intelligence 24 (2), 398-408.

Bishop, R.E.D., Parkinson, A.G., 1970. On the Planar Motion Mechanism Used in Ship Model Testing. Philosophical Transactions of the Royal Society of London. Series A, Mathematical and Physical Sciences 266 (1171), 35-61.

Boyle, P., Frean, M., 2004. Dependent gaussian processes, Advances in neural information processing systems, pp. 217-224.

Brinati, H., Neto, A.R., 1975. Application of the extended Kalman filtering to the identification of ship hydrodynamic coefficients, Proceedings of the Third Brazilian Congress of Mechanical Engineering, pp. 791-804.

Casado, M.H., Ferreiro, R., Velasco, F., 2007. Identification of nonlinear ship model parameters based on the turning circle test. Journal of Ship Research 51 (2), 174-181.

Fossen, T., Perez, T., 2004. Marine systems simulator (MSS). URL www. marinecontrol. org.

Fossen, T.I., 1994. Guidance and control of ocean vehicles. John Wiley & Sons Inc.

Fossen, T.I., 2011. Handbook of marine craft hydrodynamics and motion control. John Wiley & Sons.

Haddara, M.R., Wang, Y., 1999. Parametric identification of manoeuvring models for ships. International Shipbuilding Progress 46 (445), 5-27.

Higdon, D., 2002. Space and space-time modeling using process convolutions, Quantitative methods for current environmental issues. Springer, pp. 37-56.

Irsoy, O., Cardie, C., 2014. Deep recursive neural networks for compositionality in language, Advances in Neural Information Processing Systems, pp. 2096-2104.

Källström, C.G., Åström, K.J., Thorell, N., Eriksson, J., Sten, L., 1979. Adaptive autopilots for tankers. Automatica 15 (3), 241-254.
Kbiob, D., 1951. A statistical approach to some basic mine valuation problems on the Witwatersrand. Journal of Chemical, Metallurgical, and Mining Society of South Africa.
Kocijan, J., 2016. Modelling and Control of Dynamic Systems Using Gaussian Process Models. Springer.
Kocijan, J., Girard, A., Banko, B., Murray-Smith, R., 2005. Dynamic systems identification with Gaussian processes. Mathematical and Computer Modelling of Dynamical Systems 11 (4), 411-424.
Ljung, L., 1999. System identification. Wiley Online Library.
Luo, W., Zou, Z., 2009. Parametric identification of ship maneuvering models by using support vector machines. Journal of Ship Research 53 (1), 19-30.
Moreira, L., Soares, C.G., 2012. Recursive neural network model of catamaran manoeuvring. Int. J. Marit. Eng. RINA 154, A121-A130.
Neal, R.M., 2012. Bayesian learning for neural networks. Springer Science & Business Media.
Norrbin, N.H., 1971. Theory and observations on the use of a mathematical model for ship manoeuvring in deep and confined waters. DTIC Document.
Olsgard, F., Gray, J.S., 1995. A comprehensive analysis of the effects of offshore oil and gas exploration and production on the benthic communities of the Norwegian continental shelf. Marine Ecology Progress Series 122, 277-306.
Pettersen, K.Y., Nijmeijer, H., 2001. Underactuated ship tracking control: theory and experiments. International Journal of Control 74 (14), 1435-1446.
Son, K.-H., Nomoto, K., 1982. 5. On the Coupled Motion of Steering and Rolling of a High-speed Container Ship. Naval Architecture and Ocean Engineering 20, 73-83.
Stern, F., Agdrup, K., Kim, S., Hochbaum, A., Rhee, K., Quadvlieg, F., Perdon, P., Hino, T., Broglia, R., Gorski, J., 2011. Experience from SIMMAN 2008—the first workshop on verification and validation of ship maneuvering simulation methods, Journal of Ship Research, pp. 135-147.
Sutulo, S., Soares, C.G., 2014. An algorithm for offline identification of ship manoeuvring mathematical models from free-running tests. Ocean Engineering 79, 10-25.
Wang, X.-g., Zou, Z.-j., Yu, L., Cai, W., 2015. System identification modeling of ship manoeuvring motion in 4 degrees of freedom based on support vector machines. China Ocean Engineering 29, 519-534.
Williams, C.K., Rasmussen, C.E., 2006. Gaussian processes for machine learning.
Yoon, H.K., Rhee, K.P., 2003. Identification of hydrodynamic coefficients in ship maneuvering equations of motion by Estimation-Before-Modeling technique. Ocean Engineering 30 (18), 2379-2404.
Zhou, W., Blanke, M., 1987. Nonlinear recursive prediction error method applied to identification of ship steering dynamics.

## Acknowledgement

We thank Dr. Juš Kocijan for his assistance with the implementation of dynamic system identification with GPs and for comments that greatly improved the manuscript.

**Funding:** This research did not receive any specific grant from funding agencies in the public, commercial, or not-for-profit sectors.

## Figures Caption

Fig. 1 Definition of Body fixed coordinated system

Fig. 2 NARX for single input, single output system.

Fig. 3 NARX structure for dynamic SI of nonlinear container ships. $u1$is the measure RPM and $u2$ is the rudder angle at time $.k$..

Fig. 5 Shaft speed [rpm] and rudder angle signals for simulation of Ship

Fig. 6 Prediction from Multioutput-GPs obtained model with training data (0-700 seconds) compared to mathematical model, a) controlled surge acceleration, b) induced sway speed, c) controlled yaw speed, and d) induced roll speed

Fig. 7 Prediction from Multioutput-GPs obtained model with validation data (700-1400 seconds) compared to mathematical model, a) controlled surge acceleration, b) induced sway speed, c) controlled yaw speed, and d) induced roll speed

Fig. 8 Prediction from Multi-output GPs by algorithm of Naive Simulation with full data from input signals compared to mathematical model, a) controlled surge acceleration, b) induced sway speed, c) controlled yaw speed, and d) induced roll speed

Footnotes:

Footnote 1: https://github.com/ArizaWilmerUTAS/Multi-Output-GPs-Identification-SHIP

# Non-parametric Dynamic System Identification of Ships Using Multi-Output Gaussian Processes

Wilmer Ariza Ramirez*[1], Zhi Quan Leong[1], Hung Nguyen[1], Shantha Gamini Jayasinghe[1]

[1]Australian Maritime College, University of Tasmania, Newnham TAS 7248, Australia
Wilmer.ArizaRamirez@utas.edu.au (* Corresponding author), Z.Leong@amc.edu.au, H.D.Nguyen@utas.edu.au, shanthaj@utas.edu.au

## Abstract

A novel application of non-parametric system identification algorithm for a surface ship has been employ on this study with the aim of modelling ships dynamics with low quantity of data. The algorithm is based on multi-output Gaussian processes and its ability to model the dynamic system of a ship without losing the relationships between coupled outputs is explored. Data obtained from the simulation of a parametric model of a container ship is used for the training and validation of the multi-output Gaussian processes. The required methodology and metric to implement Gaussian processes for a 4 degrees of freedom (DoF) ship is also presented in this paper. Results show that multi-output Gaussian processes can be accurately applied for non-parametric dynamic system identification in ships with highly coupled DoF.

## Keywords

Dependent Gaussian processes; Dynamic System identification; Multi-output Gaussian processes; Non-Parametric Identification; Oceanic Vehicles

## Introduction

Dynamic modelling of oceanic vehicles including surface ships, semisubmersibles/ submersible platforms, and unmanned underwater vehicles is an active research field due to the application importance of these vessels such as goods transport, oil and gas exploration (Olsgard and Gray, 1995), underwater survey, and fishery. The common approach to modelling such vehicles is the use of Newtonian-Lagrangian mathematical models which are usually predefined. However, the presence of unaccounted dynamics caused by parametric and non-parametric uncertainties in a predefined model can increase the error between the predicted output and the real output. The cause of these uncertainties is commonly attributed to ocean currents, waves, wind, and hydrodynamic interaction with nearby structures. Since oceanic vehicles operate in dynamically changing environments performance of traditional controllers such as PID, LQR, and backstepping controllers (Fossen, 2011; Pettersen and Nijmeijer, 2001) degrade over time of operation as they require an initial offline design, calibration and are directly dependent on the predefined system parameters. An optional approach to predefined mathematical modelling is the use of non-parametric system identification (SI) methods. In this context, the application of modern machine learning algorithms that are capable of producing evolutionary adaptability to the environment has been identified as a promising approach for SI (Ljung, 1999). The present study focuses on its application for the identification of surface ship dynamics.

There are multiple mathematical models for the representation of ships dynamics. Some models are 3 DoF models where the surge, sway and yaw are represented by linear and nonlinear equations (Abkowitz, 1964; Norrbin, 1971). Other more

advanced models such as (Son and Nomoto, 1982) used a 4 DoF nonlinear model for ships including the rolling effect. The dynamic modelling of ship is a prerequisite for the design of its autopilot, navigation, steering control, and damage identification systems. The exactitude of the model can lead to the reduction of fuel consumption (Källström et al., 1979) by the correct tuning of an autopilot, better vehicle stability, and less stress over the vehicle structure (Fossen, 1994) and the possibility of advanced algorithms such as automatic ship berthing (Ahmed and Hasegawa, 2013).

Dynamic mathematical models are usually obtained by the application of Newtonian and Lagrangian mechanics, which lead to a complex system of coupled equations defined by a series of parameters. The parameters are the representation of added masses, hydrodynamics damping constants, and constants related directly with control forces such as propellers and rudders. Over the years, multiple methods have been developed to determine the hydrodynamic parameters of ships, e.g. empirical formulas, captive model test, computational fluid dynamics (CFD) calculation and parameter estimation based in SI. The most recognized and accepted method is captive model test with planar motion mechanics (Bishop and Parkinson, 1970). This method requires the use of sophisticate facilities such as towing tanks, rotating arms and planar motion mechanism to produce the required ship manoeuvres that allow the parameters to be identified. These manoeuvres can also be replicated virtually via CFD which can be a more affordable option (Stern et al., 2011). However, as the accuracy of CFD is highly dependent on the numerical settings and requires validation, physical experiments are still preferred over computational solutions.

Parameter estimation based in SI methodologies offer a practical way to identify the hydrodynamic parameters of a ship model or a complete model. The data source for

SI can be free-running model tests or full-scales trials of existing ships. SI can be categorized in two groups, parametric and non-parametric identification. Parametric identification is based on the use of numerical methods to obtain the hydrodynamics parameters of proposed mathematical models with unknown parameters. Alternatively, non-parametric identification is based on the use of single or multiple kernel functions to create a non-physics related mathematical model which is tuned by a learning procedure that uses data obtained from the original system.

Methods like Extended Kalman Filter (Åström and Källström, 1976; Brinati and Neto, 1975), Unscented Kalman Filter(Zhou and Blanke, 1987), Estimation-Before-Modelling (Yoon and Rhee, 2003), and Backstepping (Casado et al., 2007) are the most popular numerical methods for coefficient estimation. However, these methods can suffer from linearization and convergence errors. Therefore, more advanced SI methods from machine learning, e.g. neural networks (Haddara and Wang, 1999), and support vector machines (Luo and Zou, 2009) had found their space in parametric ship SI with the use of specific structures (NN) or specific selection of kernel functions(SVM), these specific structure allow the techniques to calculate some coefficients. The principal disadvantage of parametric system identification is the need of controlled test with low external perturbations and specific procedures to reduce the interference and nonlinearities between degrees of freedom.

In contrast to the parametric SI, non-parametric SI has the capacity to learn a complete model without prior knowledge of the system structure. This learning procedure leads to a simpler model with fewer parameters. Non-parametric SI brings the possibility of incorporating online learning giving the ability to improve the adaptability of the model. The capability to adapt to change is very important for application of evolutionary control techniques and damage identification. The most

recognized method of non-parametric identification for ships is recursive neural network (RNN). RNN differs over standard neural networks in the aspect that the structure of the network is organized hierarchically applying the same set of weights recursively over the structure, to produce a scalar prediction on it. (Irsoy and Cardie, 2014). This method has been used with success to identify complex ship designs like catamarans with the final purpose of offline simulation of ship behaviours (Moreira and Soares, 2012). Wang et al. (2015) presented a modified version of SVMs to capture the full coupled system in four degrees of a ship following a similar methodology to RNNs. The difference between the SVM and the neural network methods is that the SMV is less prone to overfitting, thus can reach a global optimum and require less memory. Wang's proposed a white, grey and black box system, the black box is the result of the mathematical analysis of the grey black box that leads them to recognize an applicable kernel. The drawback of neural networks and SVM machine learning methods is the lack of confident measures, and thus, an error in the prediction cannot be corrected.

Depending on the budget and availability of infrastructure and time, the parametric or non-parametric model characterization can be chosen for a given system. In the case of new designs with low complexity, the parametric identification can be carried out without inconvenience as scale model can be produced and computational CAD files are available. However, for old oceanic vehicles that require fitting of new technology, vehicles that require operation in evolving environments, and vehicles with complex designs the use of non-parametric methods can be more practical.

Nevertheless, not all possible methods of machine learning had found their way to dynamic SI of ships. If a neural network is used to generate a non-parametric model with the inclusion of the variance, the number of hidden units ideally has to be taken

to infinity, in which case it turns that a neural network with infinite hidden layers is equivalent to another machine learning method known as Gaussian Processes (Neal, 2012). GPs is a well-established method in fields such as geostatistics, where the GPs method is renamed ‘kriging’ (Kbiob, 1951). In GPs based SI the model is built over input-output data and a covariance function is used to characterise the ship behaviour. The advantage of GPs is their ability to work with small quantities of data and noisy data, and the predicted results consist of a mean and variance value. The variance of a future prediction can be used for other purposes as well such as control and model based fault detection since it contains a measure of confidence. (Kocijan et al., 2005) and (Ažman and Kocijan, 2011) described the application of GPs for the identification of nonlinear dynamics system and provided examples over simple input and single outputs systems. The standard technique of modelling multi-output systems as a combination of single output GPs has the disadvantage of not modelling the coupling relationships among the outputs of a system as a ship. A ship is a system with highly related outputs where the absence of the relation between outputs can carry to error in prediction.

In the present study, non-parametric dynamic SI for ships is proposed with the use of multi-output GPs, NARX structure and gradient descent optimization. The output from the algorithm will be a predictive value and a measure of confidence of the predictive value. Multi-output GPs is a special case of GPs with the capability to model the nonlinear behaviour and coupling among outputs of a multi-output system. Ships are ideal candidates for the use of multi-output GPs owing to their dynamic system with highly coupled outputs, i.e. the ship’s motion in 4 DoF. The present implementation was made over data obtained from a non-conventional zig-zag test with variable frequency of a 4 DoF simulated container ship. Multiple sample times

and data length were tested to find the best metric that can describe a ship. In addition to the algorithm development, another immediate objective of the study is the demonstration of the viability of GPs in modelling ships.

**Nonlinear Dynamic Ship Model**

(Son and Nomoto, 1982) proposed a 4 DoF (surge, sway, yaw and pitch) mathematical nonlinear model for ships including the contribution from hydrodynamics added masses. In respect to a body fixed frame (Fig. 1) the mathematical model can be expressed as:

$$\begin{aligned}
&\left(m+m_x\right)\dot{u}-\left(m+m_y\right)vr = X \\
&\left(m+m_y\right)v+\left(m+m_x\right)ur+m_y\alpha_y\dot{r}-m_y l_y\dot{p} = Y \\
&\left(I_x+J_x\right)\dot{p}-m_y l_y\dot{v}-m_x l_x ur = K-W\overline{GM_T}\phi \\
&\left(I_z+J_z\right)\dot{r}+m_y\alpha_y\dot{v} = N-x_G Y
\end{aligned} \tag{1}$$

Fig. 1 here

where the added mass in x-axis and y-axis are represented by $m_x$, $m_y$ and the added moment of inertia about x-axis and y-axis are represented by $J_x$ and $J_y$. The centre of added mass is denoted by the vector $\left(\alpha_x,\alpha_y,\alpha_z\right)$, while the added mass centre for $m_x$ and $m_y$ is denoted by the z-coordinates of $l_x$ and $l_y$. The vector $[X,Y,K,N]$ expresses the forces over the vehicle and can be defined as:

$$
\begin{aligned}
X &= X(u) + (1-t)T + X_{vr}vr + X_{vv}v^2 + X_{rr}r^2 \\
&\quad + X_{\phi\phi}\phi^2 + X_{\delta}\sin(\delta) + c_{RX}F_N \sin\delta \\
\\
Y &= Y_v v + Y_r r + Y_\phi \phi + Y_p p + Y_{vvv}v^3 + Y_{rrr}r^3 \\
&\quad + Y_{vvr}v^2 r + Y_{vrr}vr^2 + Y_{vv\phi}v^2\phi + Y_{v\phi\phi}v\phi^2 \\
&\quad + Y_{rr\phi}r^2\phi + Y_{r\phi\phi}r\phi^2 + Y_{\delta}\cos(\delta) \\
&\quad - (1+a_H)\, z_R F_N \cos\delta \\
\\
K &= K_v v + K_r r + K_\phi \phi + K_p p + K_{vvv}v^3 + K_{rrr}r^3 \\
&\quad + K_{vvr}v^2 r + K_{vrr}vr^2 + K_{vv\phi}v^2\phi + K_{v\phi\phi}v\phi^2 \\
&\quad + K_{rr\phi}r^2\phi + K_{r\phi\phi}r\phi^2 + K_{\delta}\cos(\delta) \\
&\quad + (1+a_H)\, F_N \cos\delta \\
\\
N &= N_v v + N_r r + N_\phi \phi + N_p p + N_{vvv}v^3 + N_{rrr}r^3 \\
&\quad + N_{vvr}v^2 r + N_{vrr}vr^2 + N_{vv\phi}v^2\phi + N_{v\phi\phi}v\phi^2 \\
&\quad + N_{rr\phi}r^2\phi + N_{r\phi\phi}r\phi^2 + N_{\delta}\cos(\delta) \\
&\quad + (x_R + a_H x_H)\, z_R F_N \cos\delta
\end{aligned}
\tag{2}
$$

where:

$X(u)$ = function dependent on the velocity $X_{|u|u}|u|u$

$\delta$ = rudder angle

$F_N$ =rudder force

$X_{vr}X_{vv},...N_{r\phi\phi}$ =model parameters

As can be seen, the mathematical model is defined by more than 50 parameters including parameters from the actuation surfaces. An example of the hydrodynamic parameters and its application can be found in Fossen (1994).

**Dynamic Identification with Multi-output GPs**

The design of the algorithm for multi-output SI with GPs is based on the previous work of Kocijan (2016). The dynamic identification problem can be defined as the search for relation between a vector formed by delayed samples from the inputs $u(k)$ and outputs $y(k-1)$ and the future output values. The relationship can be expressed by the equation:

$$\mathbf{y}(k+1) = f\left(\mathbf{z}(k), \boldsymbol{\Theta}\right) + v(k) \tag{3}$$

where $f\left(\mathbf{z}(k), \boldsymbol{\Theta}\right)$ is a function that maps the sample data vector $\mathbf{z}(k)$ that contains the vector $[\mathbf{u}(k-1), \mathbf{y}(k-1)]$ to the output space based on the hyperparameters $\boldsymbol{\Theta}$. $\mathbf{v}(k)$ accounts for the noise and error in the prediction of output $\mathbf{y}(k)$. In the case of dynamic SI, the discrete time variable $(k)$ is presented as an embedded element in the regression process as it is accounted in the delayed samples.

A requirement for dynamic SI of nonlinear systems is the selection of a nonlinear model structure as nonlinear autoregressive model with exogenous input (NARX), nonlinear autoregressive (NAR), nonlinear output-error (NOE), nonlinear finite-impulse response (NFIR), etc. From all the possible structures, the simpler and most popular structure to implement is NARX as its predictions are based on previous measurements of the input signals and output signals and require a more simplified optimization scheme. In the case of a ship, NARX is the most practical configuration since the measuring points are restricted to the available sensors. Fig. 2 shows the NARX configuration for Dynamic GPs for a simple case of one-input one-output system.

Fig. 2 here

In the case of a single-input single-output structure NARX for a GPs, the inputs signals are not considered separately as they are grouped into a single vector of dimension $n$ that derives to an output of single dimension. In the case of a four DoF ship, the system can be defined a function $f$ who depends of a vector formed by the respective regressors of each output and the regressors of the command signals of propeller and rudder such as.

$$\mathbf{y} = f\left(\mathbf{y}_{(k-1:n)}, \mathbf{u}_{RPM\,(k-1:n)}, \mathbf{u}_{rudder\,(k-1:n)}\right)$$

If a Newton-Lagrange mathematical model had been used, our system will have two-input signals, four-output system signals. (Fig. 3) presents the graphical representation of the NARX architecture used with multi-output GPs with four vector of dimension R3.

Fig. 3 Here

**Multi-output GPs**

The previous sections outline Eq.(1) and Eq.(2) which show the level of coupling between the Newton-Lagrange equations of a ship. The nonlinearity and coupling between outputs are better represented by a multi-output GPs. multi-output GPs presented here is based on the work of Alvarez and Lawrence (2009). multi-output GPs are founded in the regression of data by the convolution of white noise process with a smoothing function(Higdon, 2002). This was later introduced by Boyle and Frean (2004) to the machine learning community by assuming multiple latent process defined over a space $\Re^q$. The dependency between two outputs is modelled with a common latent process and their independency with a latent function who does not interact with other outputs. If a set of functions $\left\{f_q(\mathbf{x})\right\}_{q=1}^{Q}$ is considered,

where $Q$ is the Output Dimension for a $N$ number of data points, where each function is expressed as the convolution between a smoothing kernel $\{k_q(\mathbf{x})\}_{q=1}^{Q}$ and a latent function $\mathbf{u}(z)$ ,

$$f_q(x) = \int_{-\infty}^{\infty} k_q(\mathbf{x}-\mathbf{z})u(\mathbf{z})d\mathbf{z} \tag{4}$$

This equation can be generalized for more than one latent function $\{u_r(\mathbf{x})\}_{r=1}^{R}$ and include a corruption function (noise) independent to each of the outputs $w_q(\mathbf{x})$, to obtain

$$\begin{aligned}\mathbf{y}_q(\mathbf{x}) &= f_q(\mathbf{x}) + w_q(\mathbf{x}) \\ \mathbf{y}_q(\mathbf{x}) &= \sum_{r=1}^{R}\int_{-\infty}^{\infty} k_{qr}(\mathbf{x}-\mathbf{z})u_r(\mathbf{z})d\mathbf{z} + w_q(\mathbf{x})\end{aligned} \tag{5}$$

The covariance between two different functions $y_q(x)$ and $y_s(x')$ is:

$$\begin{aligned}\operatorname{cov}\left[\mathbf{y}_q(\mathbf{x}),\mathbf{y}_s(\mathbf{x}')\right] &= \operatorname{cov}\left[f_q(\mathbf{x}),f_s(\mathbf{x}')\right] \\ &\quad + \operatorname{cov}\left[w_q(\mathbf{x}),w_s(\mathbf{x}')\right]\delta_{qs}\end{aligned} \tag{6}$$

where

$$\begin{aligned}\operatorname{cov}\left[f_q(\mathbf{x}),f_s(\mathbf{x}')\right] &= \sum_{r=1}^{R}\sum_{p=1}^{R}\int_{-\infty}^{\infty} k_{qr}(\mathbf{x}-\mathbf{z}) \\ &\quad \int_{-\infty}^{\infty} k_{sp}(\mathbf{x}'-\mathbf{z}')\operatorname{cov}\left[u_r(\mathbf{z}),u_p(\mathbf{z}')\right]d\mathbf{z}'d\mathbf{z}\end{aligned} \tag{7}$$

If it is assumed that $u_r(\mathbf{z})$ is an independent white noise $\operatorname{cov}\left[u_r(\mathbf{z}),u_p(\mathbf{z}')\right] = \sigma_{ur}^2\delta_{rp}\delta_{z,z'}$ , Equation (7) will become:

$$\operatorname{cov}\left[f_q(\mathbf{x}),f_s(\mathbf{x}')\right] = \sum_{r=1}^{R}\sigma_{ur}^2\int_{-\infty}^{\infty} k_{qr}(\mathbf{x}-\mathbf{z})k_{sp}(\mathbf{x}'-\mathbf{z}')d\mathbf{z} \tag{8}$$

The mean $\hat{\mathbf{y}}'$ with variance $\boldsymbol{\sigma}_{\hat{\mathbf{y}}'}$ of a predictive distribution at the point $\mathbf{x}'$ given the hyperparameters $\boldsymbol{\Theta}$ can be defined as

$$\hat{\mathbf{y}}' = k(\mathbf{x}', \mathbf{x})k(\mathbf{x}, \mathbf{x})^{-1}\mathbf{y} \tag{9}$$

and variance

$$\boldsymbol{\sigma}^2_{\hat{y}'} = k(\mathbf{x}', \mathbf{x}') - k(\mathbf{x}', \mathbf{x})^T k(\mathbf{x}, \mathbf{x})^{-1} k(\mathbf{x}', \mathbf{x}) \tag{10}$$

A complete explanation over the convolution process can be found in (Alvarez and Lawrence, 2009) and a complete implementation in Alvarez and Lawrence (2014).

**Learning Hyperparameters**

There are two principal methods for learning the hyperparameters $\Theta$, Bayesian model interference and marginal likelihood. Bayesian inference is based on the assumption that a prior data of the unknown function to be mapped is known. A posterior distribution over the function is refined by incorporation of observations. The marginal likelihood method is based on the aspect that some hyperparameters are going to be more noticeable. Over this base the posterior distribution of hyperparameters can be described with a unimodal narrow Gaussian distribution.

The learning of GPs hyperparameters $\Theta$ is commonly done by the maximization of the marginal likelihood. The marginal likelihood can be expressed as:

$$p\left(\mathbf{y}|\mathbf{x}, \boldsymbol{\Theta}\right) = \frac{1}{(2\pi)^{\frac{N}{2}}|\mathbf{K}|^{\frac{1}{2}}} e^{-\frac{1}{2}\mathbf{y}^T\mathbf{K}^{-1}\mathbf{y}} \tag{11}$$

where $\mathbf{K}$ is the covariance matrix, $N$ is the number of input learning data points and $y$ is a vector of learning output data of the form $\left[y_1; y_2; \cdots y_N\right]$. To reduce the

calculation complexity, it is preferred to use the logarithmical marginal likelihood that is obtained by the application of logarithmic properties to (11).

$$\mathcal{L}(\boldsymbol{\Theta}) = -\frac{1}{2}\log(|\mathbf{K}|) - \frac{1}{2}\mathbf{y}^T\mathbf{K}^{-1}\mathbf{y} - \frac{N}{2}\log(2\pi) \tag{12}$$

To find a solution for the maximization of log-likelihood multiples methods of optimization can be applied, like, particle swarm optimization, genetic algorithms, or gradient descent. For deterministic optimization methods, the computation of likelihood partial derivatives with respect to each hyperparameter is require. From (Williams and Rasmussen, 2006, p. 114) log-likelihood derivatives for each hyperparameter can be calculated by:

$$\frac{\partial\mathcal{L}(\boldsymbol{\Theta})}{\partial\boldsymbol{\Theta}_i} = -\frac{1}{2}trace\left(\mathbf{K}^{-1}\frac{\partial\mathbf{K}}{\partial\boldsymbol{\Theta}_i}\right) + \frac{1}{2}\mathbf{y}^T\mathbf{K}^{-1}\frac{\partial\mathbf{K}}{\partial\boldsymbol{\Theta}_i}\mathbf{K}^{-1} \tag{13}$$

Equation (12) gives us the learning process computational complexity, for each cycle the inverse of the covariance matrix of $\mathbf{K}$ has to be calculated. This calculation carries a complexity $\mathbf{O}(\mathbf{NM})^3$ where $N$ is the number of data points and $M$ is the number of outputs of the system. After learning, the complexity of predicting the value $\mathbf{y}(k+1)$ is $\mathbf{O}(\mathbf{NM})$ and to predict the mean value $\boldsymbol{\sigma}(k+1)$ is $\mathbf{O}(\mathbf{NM})^2$ .The higher training complexity $\mathbf{O}(\mathbf{NM})^3$ is the major disadvantage of using multi-output GPs. If the number of data increases the complexity of learning the hyperparameters increases in a cubic form. Methods such as genetic algorithms, differential equations, and particle swarm optimization can be applied to avoid the calculation of the marginal likelihood partial derivatives and thereby reduce the computational time.

## Experiment Setup and Results

### Experiment setup

The implementation of Son and Nomoto (1982) mathematical model of a container ship programmed in the Marine Systems Simulator (Fossen and Perez, 2004) was used to create the required databases. The container ship particulars can be found in Table 1. A simulation setup was developed in MATLAB/Simulink to emulate the behaviour of a container ship (Fig. 4). 1400 seconds were simulated where the inputs signals are constant shaft speed in RPM and a cosine signal with frequency change for rudder angle in radians (Fig. 5). The objective of not using a standard test as zigzag or turning circle is to test the ability of GPs for online learning. A sample data point was captured for each three steps over the input and outputs. A total of 1868 points were captured over four outputs and 934 point over two input signals. The data set was divided in two sets of points, the first set of points is used for the model learning, and the second set of points is used for learning validation. The Validation data is purposely chosen to be beyond the range of training data to test the ability of the method to predict beyond the training range. Two neural network nonlinear system identification models were also prepared. The first system (RNN1) was a recurrent neural network system and it has a similar architecture to the Multi-output GPs $f\left[\mathbf{y}_{(k-1)}, \mathbf{u}_{RPM\,(k-1:2)}, \mathbf{u}_{rudder\,(k-1:2)}\right]$ for each output. The second NN system (NN2) use a common NARX identification methodology and used the last four delayed outputs of the system and the last delayed input commands $f\left[\mathbf{y}_{(k-1:4)}, \mathbf{u}_{1(k-1:2)}, \mathbf{u}_{2(k-1:2)}\right]$ for each output. The neural network systems use a Log-sigmoid transfer function, at different of GPs the training of NN was done by Levenberg-Marquardt backpropagation. Both neural network systems were trained, validated, and tested with the same data used for the multi-output GPs. The complete implementation code can be found at the GitHub Repository (FOOTNOTE 1).

Table 1 Particulars of Container Ship

| Parameter | Magnitude | |
|---|---|---|
| Length overall | 175 | m |
| Breadth | 25.4 | m |
| Max. Rudder Angle | 10 | deg. |
| Max. shaft velocity | 160 | Rpm |
| Displacement Volume | 21222 | $m^3$ |
| Rudder Area | 33.0376 | $m^2$ |
| Propeller diameter | 6.533 | m |

Fig. 4 Here

Fig. 5 Here

**Training and validation**

The software written by Alvarez and Lawrence (2014) was softly modified to accept the multidimensional input vectors and a script was written to implement the NARX structure. The convolution of two square exponential Gaussian processes and a white noise was chosen as kernel. The inputs of the GPs were defined as four inputs of dimension five of the form:

$$\begin{bmatrix} \dot{u}_k \\ v_k \\ r_k \\ p_k \end{bmatrix} = f\left(\mathbf{y}_{k-1}, \mathbf{u}_{RPM\,(k-1:2)}, \mathbf{u}_{rudder\,(k-1:2)}\right) \tag{14}$$

where $\mathbf{y}_{k-1}$ is the first regressor of the output vector $[\dot{u}_k, v_k, r_k, p_k]$.

The selection of the structure of regressors was determined via the examination of the mathematical model. Each output is affected by the past states of output and rudder force $F_N$ produced by the interaction of the rudder angle and the propeller RPM as both signals are required for the calculation of $F_N$. Under this assumption different structures were tested to verify the responsiveness to each regressor. The test showed that the container ship system is more responsive to regressors from the rudder angle and the propeller RPM.

The captured output vector was the derivative of surge speed, the speed in sway and the angular speeds of yaw and roll, $[\dot{u}, v, r, p]$. As can be seen in eq.(1) and eq.(2) the surge speed is not highly couple to the other system outputs, in our simulation capturing the surge speed and posterior simulation was not converging to the real output, in contrast the surge speed derivative shows coupling with other system outputs. The input signals and outputs were normalized between -1 and 1 to give all the inputs and outputs the same weight in the learning process.

For the training, the minimization of the negative logarithmical likelihood was used along with the scaled conjugate gradient with multiple start points to insure convergence. Fig. 6 shows the results of GPs training compared to the real system signals, and the error plots between the predicted and real systems. In all the graphs, a confidence band $2\sigma$ is plotted. The error for the surge derivative is less than 0.02 over the training data.

Fig. 6a Here

Fig. 6b Here

Fig. 6c Here

Fig. 6d Here

The validation data consisted of the real output from the training data with the system delay $(k-1)$ in vector form with the delayed commanded inputs. The segments of results from the validation with the second set of data are depicted in Fig. 7, the predicted output and confidence of $2\sigma$ band is portrayed in comparison to the original system. The low validation errors show a good system prediction for the sway speed and yaw speed. It can be notice that the simulation precision is lose by how far from the training data the step is. The variance in our validation results increase as the data used for validation drift away from the trained operational region.

This was done with the objective to test the capability of GPs to predict outside the trained operational region.

Fig. 7a Here

Fig. 7b Here

Fig. 7c Here

Fig. 7d Here

**Simulation**

A third step was implemented in the way of a naive simulation. Methods of control with non-parametric models require a number of step forward of prediction to be able to control a system. With the objective of testing the ability to predict a system from past data, a naive simulation was setup. At each step the output from the simulation is feedback to the simulation as the past input $y_i(k-1)$, the initial position and control signal of rudder and forward speed where used, the naive simulation covers training(0-700s) and validation data(701-1400s) acquired from the original simulation. Table 2 shows the root mean square error (RMSE), the predicted residual error sum of squares (PRESS) measurements for the simulation stage over the training and validation data, and the training time and step simulation time for each of the methodologies. The RMSE and PRESS value for the proposed GPs are smaller than the other systems. As evident in Fig. 8(a-c) NNARX system with the same architecture (marked as NarxNN) and data as in the multi output GPs has limitations in the capability to predict the system behaviour beyond the training range in all DoF. The more complex RNN system (RNN1) produces relatively good results, except in predicting the surge. This is evident Fig. 8 (a) where RNN1 results in large deviations

from the original system, especially after 1000s.The yaw output in Fig. 8 (c) shows a higher variance as results of higher association to the other outputs of the system and similitude to other training data this is because of normalization of the outputs in the training data. The difference in capability of prediction of the system is related to their internal functions and how they relate the training data. In comparison to NNRX and RNN, the multi-output GPs show similar performance than RNN outside the training horizon in all the DoF. This is evident in all the results shown in Fig. 8 with the close match to the system from the simulation, it can be established that the Gaussian model can be used for applications as control and failure detection as it can predict future system states with the added value of a confidence measure.

Table 2 Summary prediction quality measurements

| | **GPs** | **NarxNN** | **RNN1** |
|---|---|---|---|
| **RMSE** | 0.0091 | 0.0092 | 0.044 |
| **PRESS** | 0.2327 | 5.47 | 0.2382 |
| **Training time(s)** | 779 | 245 | 125 |
| **Step simulation time** | 0.0625 | 0.032 | 0.027 |

Fig. 8a Here

Fig. 8b Here

Fig. 8c Here

Fig. 8d Here

## Conclusion

The basic methodology for the use of multiple-output Gaussian distribution for the identification of ships dynamical models is presented in this paper. The methodology has been validated with the data obtained from a coupled dynamical system of a container ship. With the proposed Gaussian model, the large number of system parameters found in a typical ship model can be reduced to a smaller number of hyperparameters. A standard validation process of machine learning and prediction

over the complete data set of training and validation were executed to establish the model quality and robustness of the algorithm. The prediction of the full set of data based in a start value and feedback from the last prediction step show low error. As the results indicate, multi-output GPs has the ability to model complex dynamic system having highly coupled outputs and provide a measure of the confidence represented by the variance.

The use of other methods such as sparse multi-output GPs and the use of more powerful prediction techniques as Taylor series or Montecarlo method can take advantage of the variance to increase the horizon of cover manoeuvres and the prediction accuracy. Although the results obtained look encouraging, conclusion about the practical value of the method can only be obtained by comparison with other GPs methods and validation with real data from a ship or other oceanic vehicle.

## References


Abkowitz, M.A., 1964. Lectures on ship hydrodynamics--Steering and manoeuvrability.

Ahmed, Y.A., Hasegawa, K., 2013. Automatic ship berthing using artificial neural network trained by consistent teaching data using nonlinear programming method. Engineering Applications of Artificial Intelligence 26 (10), 2287-2304.

Alvarez, M., Lawrence, N., 2014. Multiple output Gaussian processes in MATLAB, Github, GitHub repository.

Alvarez, M., Lawrence, N.D., 2009. Sparse convolved Gaussian processes for multi-output regression, Advances in neural information processing systems, pp. 57-64.

Åström, K.J., Källström, C., 1976. Identification of ship steering dynamics. Automatica 12 (1), 9-22.

Ažman, K., Kocijan, J., 2011. Dynamical systems identification using Gaussian process models with incorporated local models. Engineering Applications of Artificial Intelligence 24 (2), 398-408.

Bishop, R.E.D., Parkinson, A.G., 1970. On the Planar Motion Mechanism Used in Ship Model Testing. Philosophical Transactions of the Royal Society of London. Series A, Mathematical and Physical Sciences 266 (1171), 35-61.

Boyle, P., Frean, M., 2004. Dependent gaussian processes, Advances in neural information processing systems, pp. 217-224.

Brinati, H., Neto, A.R., 1975. Application of the extended Kalman filtering to the identification of ship hydrodynamic coefficients, Proceedings of the Third Brazilian Congress of Mechanical Engineering, pp. 791-804.

Casado, M.H., Ferreiro, R., Velasco, F., 2007. Identification of nonlinear ship model parameters based on the turning circle test. Journal of Ship Research 51 (2), 174-181.

Fossen, T., Perez, T., 2004. Marine systems simulator (MSS). URL www. marinecontrol. org.

Fossen, T.I., 1994. Guidance and control of ocean vehicles. John Wiley & Sons Inc.

Fossen, T.I., 2011. Handbook of marine craft hydrodynamics and motion control. John Wiley & Sons.

Haddara, M.R., Wang, Y., 1999. Parametric identification of manoeuvring models for ships. International Shipbuilding Progress 46 (445), 5-27.

Higdon, D., 2002. Space and space-time modeling using process convolutions, Quantitative methods for current environmental issues. Springer, pp. 37-56.

Irsoy, O., Cardie, C., 2014. Deep recursive neural networks for compositionality in language, Advances in Neural Information Processing Systems, pp. 2096-2104.

Källström, C.G., Åström, K.J., Thorell, N., Eriksson, J., Sten, L., 1979. Adaptive autopilots for tankers. Automatica 15 (3), 241-254.
Kbiob, D., 1951. A statistical approach to some basic mine valuation problems on the Witwatersrand. Journal of Chemical, Metallurgical, and Mining Society of South Africa.
Kocijan, J., 2016. Modelling and Control of Dynamic Systems Using Gaussian Process Models. Springer.
Kocijan, J., Girard, A., Banko, B., Murray-Smith, R., 2005. Dynamic systems identification with Gaussian processes. Mathematical and Computer Modelling of Dynamical Systems 11 (4), 411-424.
Ljung, L., 1999. System identification. Wiley Online Library.
Luo, W., Zou, Z., 2009. Parametric identification of ship maneuvering models by using support vector machines. Journal of Ship Research 53 (1), 19-30.
Moreira, L., Soares, C.G., 2012. Recursive neural network model of catamaran manoeuvring. Int. J. Marit. Eng. RINA 154, A121-A130.
Neal, R.M., 2012. Bayesian learning for neural networks. Springer Science & Business Media.
Norrbin, N.H., 1971. Theory and observations on the use of a mathematical model for ship manoeuvring in deep and confined waters. DTIC Document.
Olsgard, F., Gray, J.S., 1995. A comprehensive analysis of the effects of offshore oil and gas exploration and production on the benthic communities of the Norwegian continental shelf. Marine Ecology Progress Series 122, 277-306.
Pettersen, K.Y., Nijmeijer, H., 2001. Underactuated ship tracking control: theory and experiments. International Journal of Control 74 (14), 1435-1446.
Son, K.-H., Nomoto, K., 1982. 5. On the Coupled Motion of Steering and Rolling of a High-speed Container Ship. Naval Architecture and Ocean Engineering 20, 73-83.
Stern, F., Agdrup, K., Kim, S., Hochbaum, A., Rhee, K., Quadvlieg, F., Perdon, P., Hino, T., Broglia, R., Gorski, J., 2011. Experience from SIMMAN 2008—the first workshop on verification and validation of ship maneuvering simulation methods, Journal of Ship Research, pp. 135-147.
Sutulo, S., Soares, C.G., 2014. An algorithm for offline identification of ship manoeuvring mathematical models from free-running tests. Ocean Engineering 79, 10-25.
Wang, X.-g., Zou, Z.-j., Yu, L., Cai, W., 2015. System identification modeling of ship manoeuvring motion in 4 degrees of freedom based on support vector machines. China Ocean Engineering 29, 519-534.
Williams, C.K., Rasmussen, C.E., 2006. Gaussian processes for machine learning.
Yoon, H.K., Rhee, K.P., 2003. Identification of hydrodynamic coefficients in ship maneuvering equations of motion by Estimation-Before-Modeling technique. Ocean Engineering 30 (18), 2379-2404.
Zhou, W., Blanke, M., 1987. Nonlinear recursive prediction error method applied to identification of ship steering dynamics.

## Acknowledgement

We thank Dr. Juš Kocijan for his assistance with the implementation of dynamic system identification with GPs and for comments that greatly improved the manuscript.

**Funding:** This research did not receive any specific grant from funding agencies in the public, commercial, or not-for-profit sectors.

## Figures Caption

Fig. 1 Definition of Body fixed coordinated system

Fig. 2 NARX for single input, single output system.

Fig. 3 NARX structure for dynamic SI of nonlinear container ships. $u1$is the measure RPM and $u2$ is the rudder angle at time $.k$..

Fig. 5 Shaft speed [rpm] and rudder angle signals for simulation of Ship

Fig. 6 Prediction from Multioutput-GPs obtained model with training data (0-700 seconds) compared to mathematical model, a) controlled surge acceleration, b) induced sway speed, c) controlled yaw speed, and d) induced roll speed

Fig. 7 Prediction from Multioutput-GPs obtained model with validation data (700-1400 seconds) compared to mathematical model, a) controlled surge acceleration, b) induced sway speed, c) controlled yaw speed, and d) induced roll speed

Fig. 8 Prediction from Multi-output GPs by algorithm of Naive Simulation with full data from input signals compared to mathematical model, a) controlled surge acceleration, b) induced sway speed, c) controlled yaw speed, and d) induced roll speed

Footnotes:

Footnote 1: https://github.com/ArizaWilmerUTAS/Multi-Output-GPs-Identification-SHIP

**Figure 1**

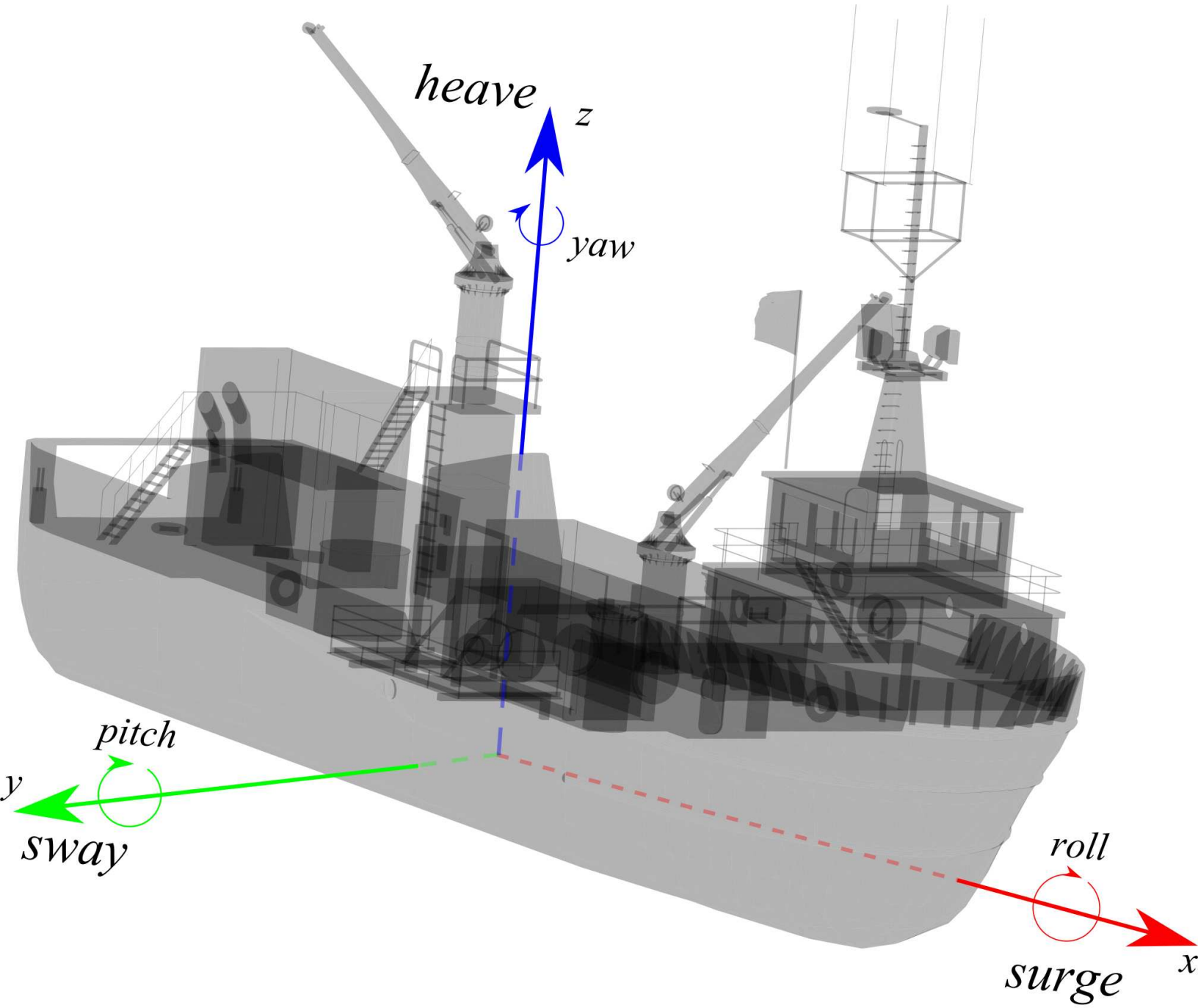

**Figure 4**

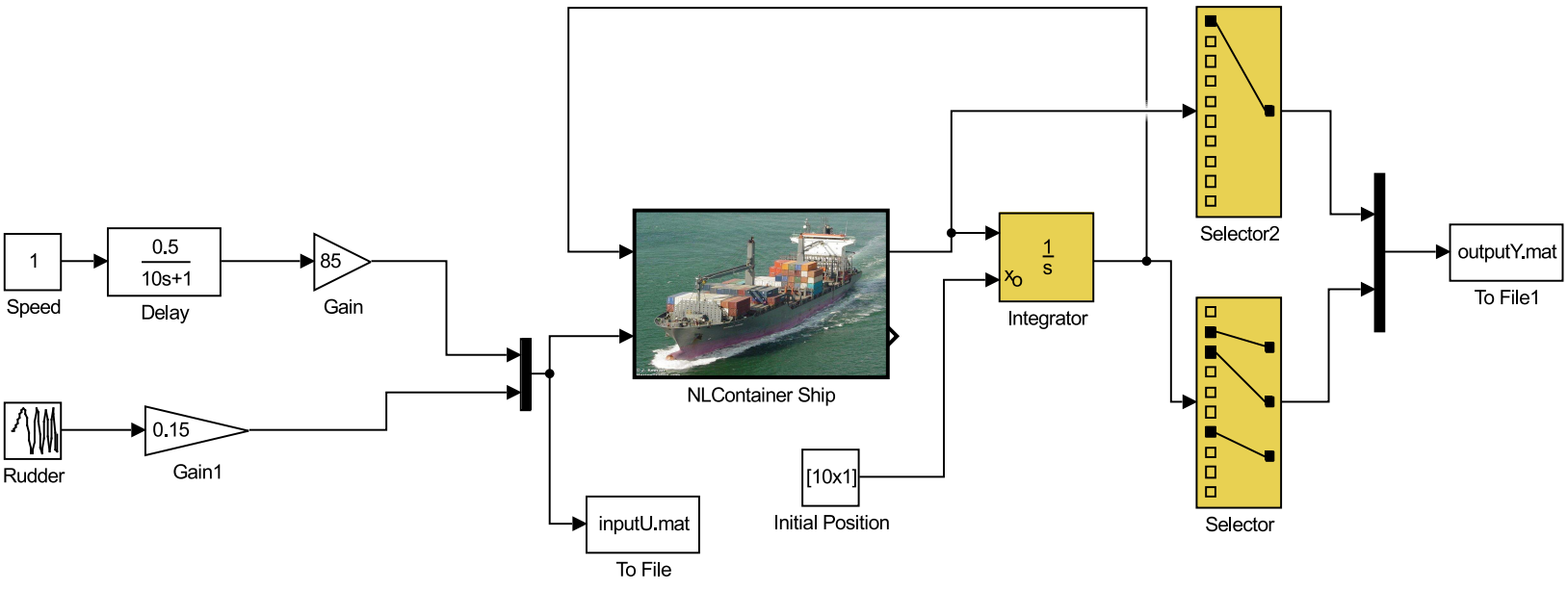
1
Speed
0.5
10s+1
Delay
85
Gain
0.15
Gain1
Rudder
NLContainer Ship
inputU.mat
To File
[10x1]
Initial Position
1
s
Integrator
Selector2
Selector
outputY.mat
To File1

**Figure 5**

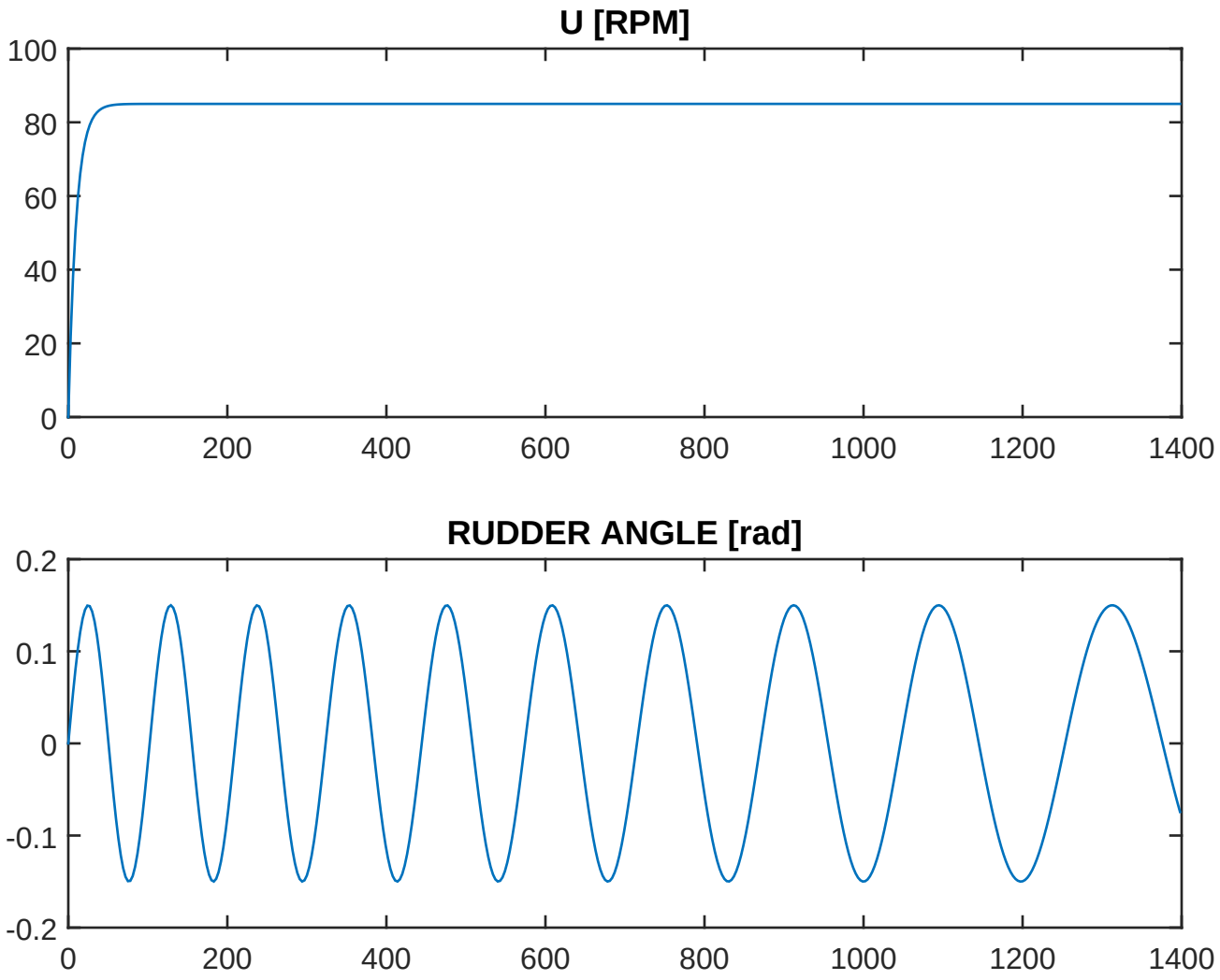
U [RPM]
100
80
60
40
20
0
0
200
400
600
800
1000
1200
1400
RUDDER ANGLE [rad]
0.2
0.1
0
-0.1
-0.2
0
200
400
600
800
1000
1200
1400

Figure 2

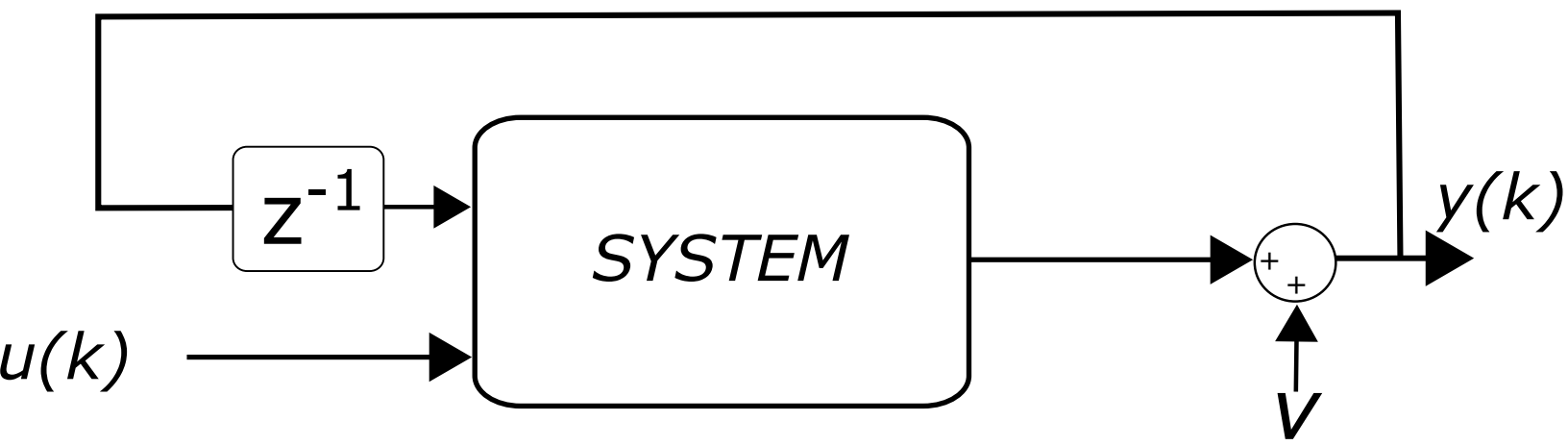

Figure 3

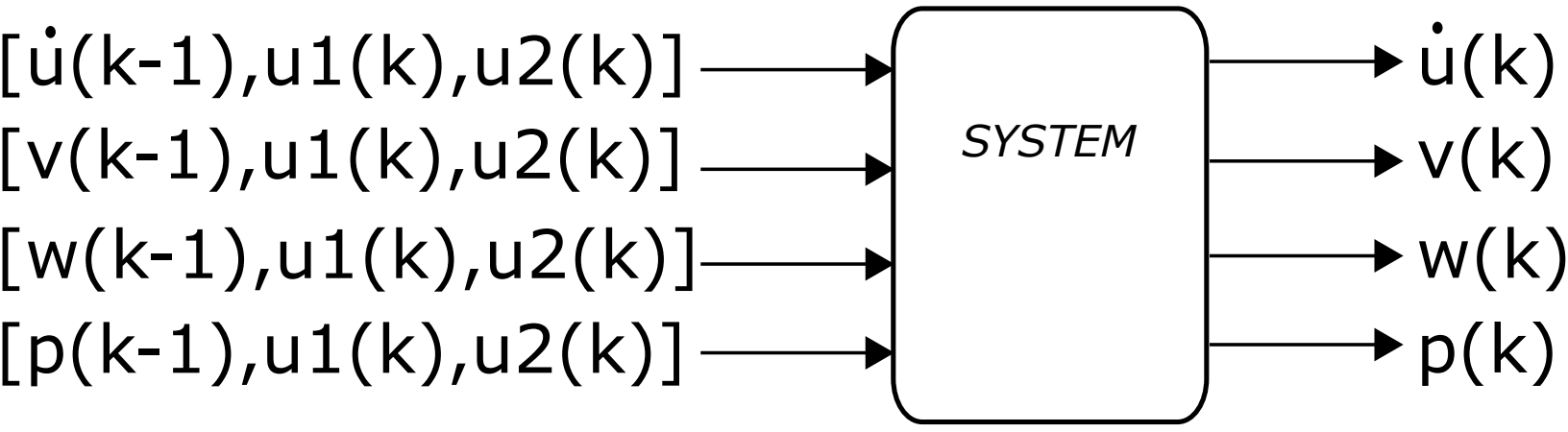
[u̇(k-1),u1(k),u2(k)]
[v(k-1),u1(k),u2(k)]
[w(k-1),u1(k),u2(k)]
[p(k-1),u1(k),u2(k)]
SYSTEM
u̇(k)
v(k)
w(k)
p(k)

**Figure 6 a**

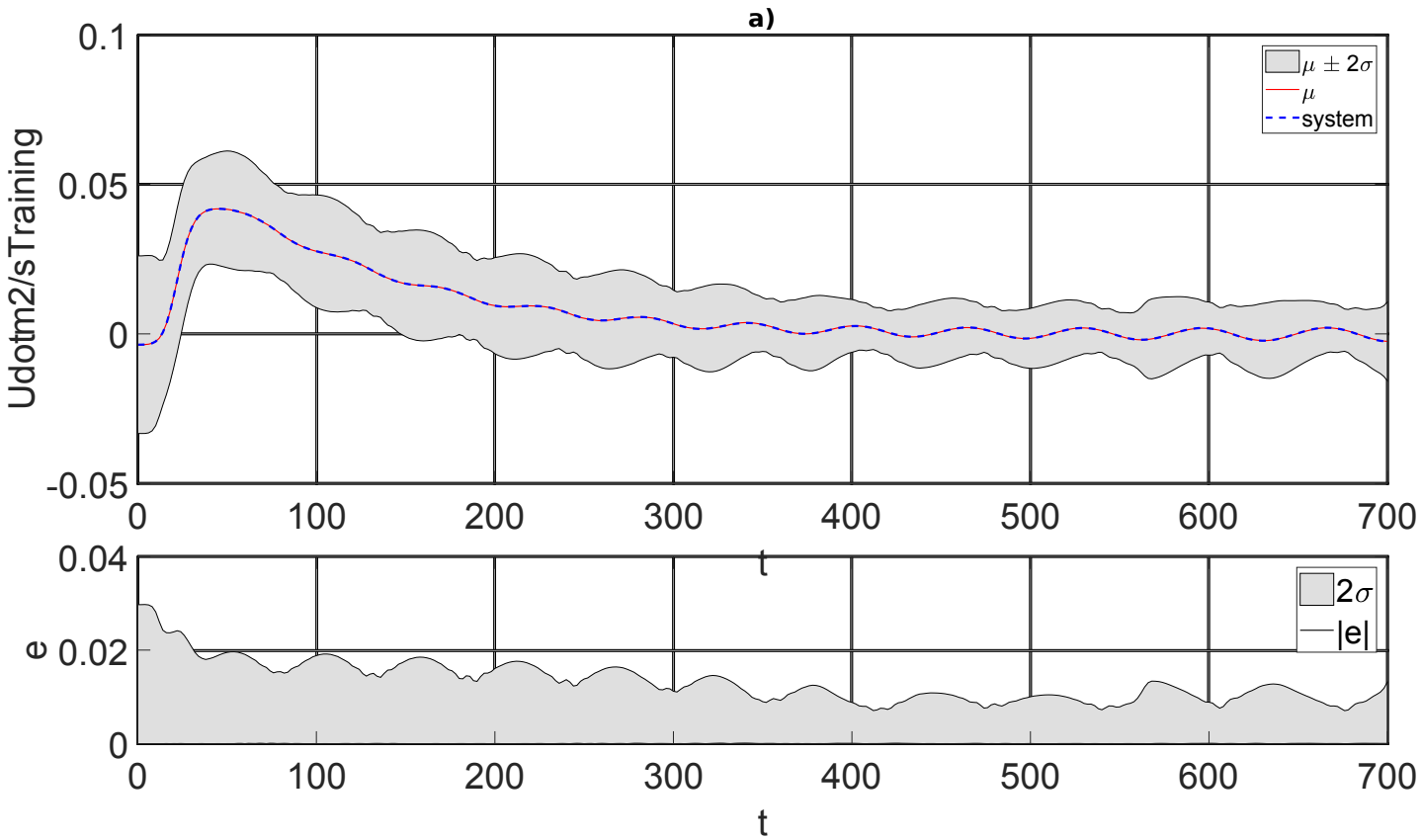
a)
0.1
0.05
0
-0.05
Udotm2/sTraining
$\mu \pm 2\sigma$
$\mu$
system
0
100
200
300
400
500
600
700
t
0.04
0.02
0
e
$2\sigma$
|e|
0
100
200
300
400
500
600
700
t

**Figure 6 b**

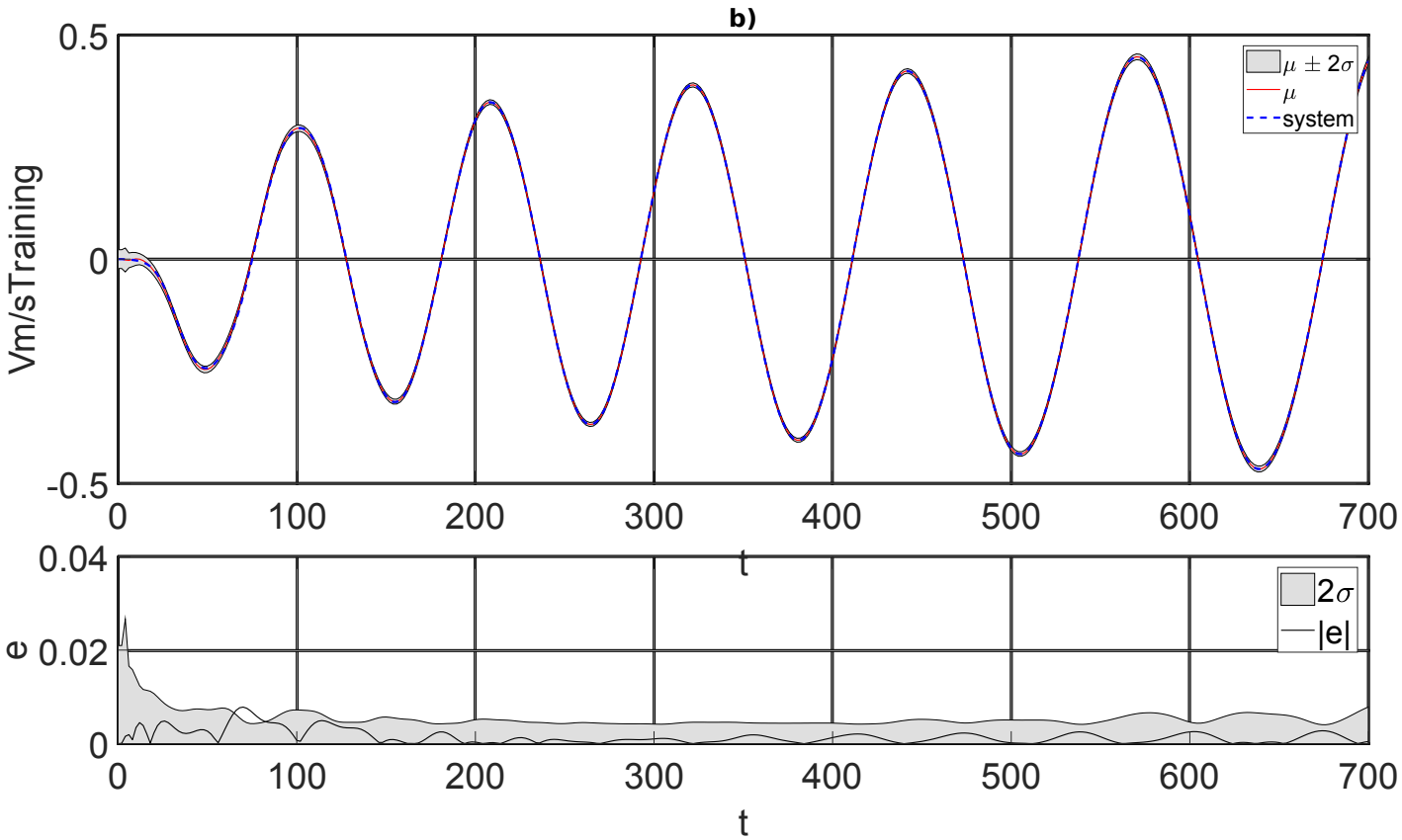
b)
0.5
0
-0.5
Vm/sTraining
$\mu \pm 2\sigma$
$\mu$
system
0
100
200
300
400
500
600
700
t
0.04
0.02
0
e
$2\sigma$
|e|
0
100
200
300
400
500
600
700
t

**Figure 6 c**

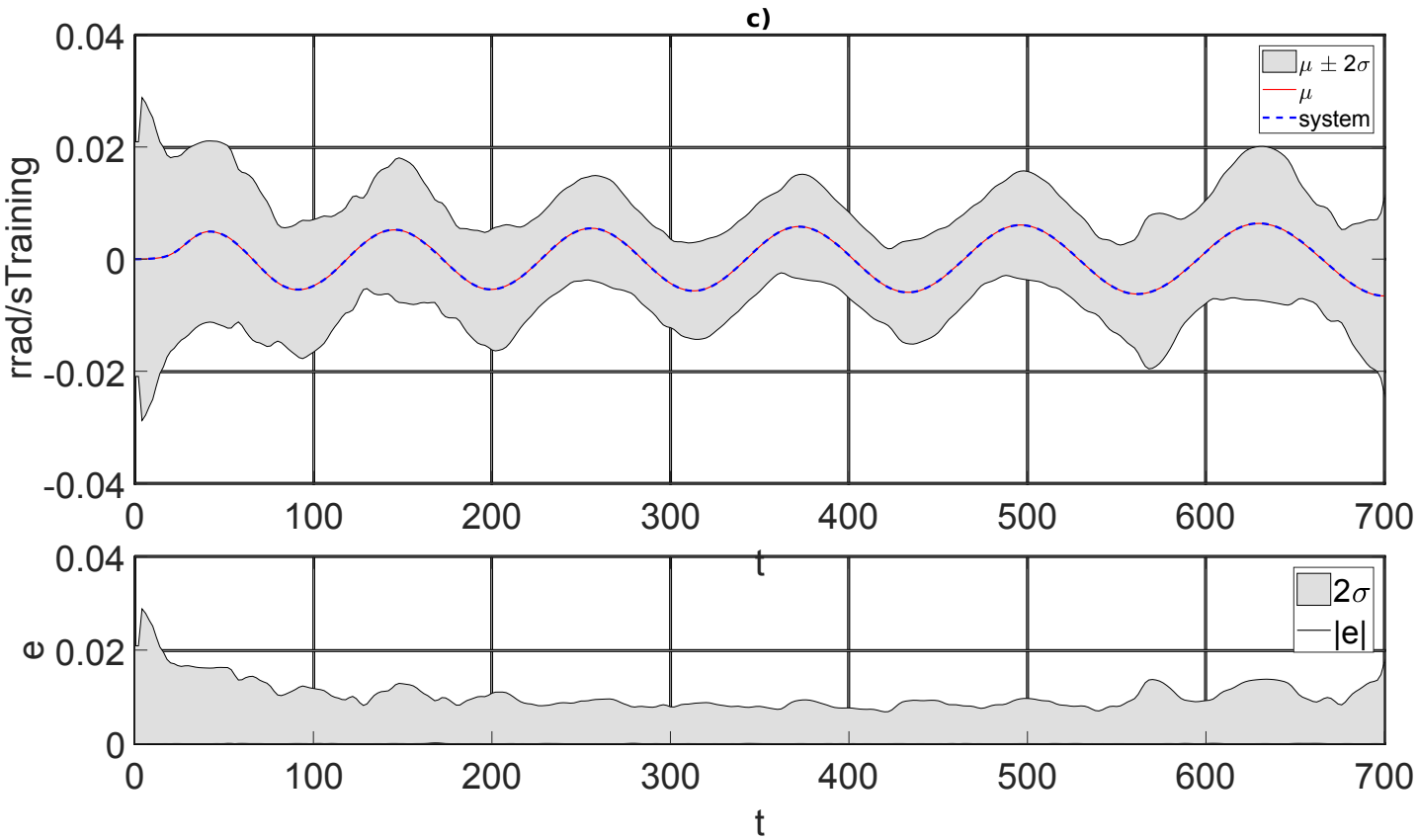
c)
0.04
0.02
0
-0.02
-0.04
rrad/sTraining
$\mu \pm 2\sigma$
$\mu$
system
0
100
200
300
400
500
600
700
t
0.04
0.02
0
e
$2\sigma$
|e|
0
100
200
300
400
500
600
700
t

**Figure 6 d**

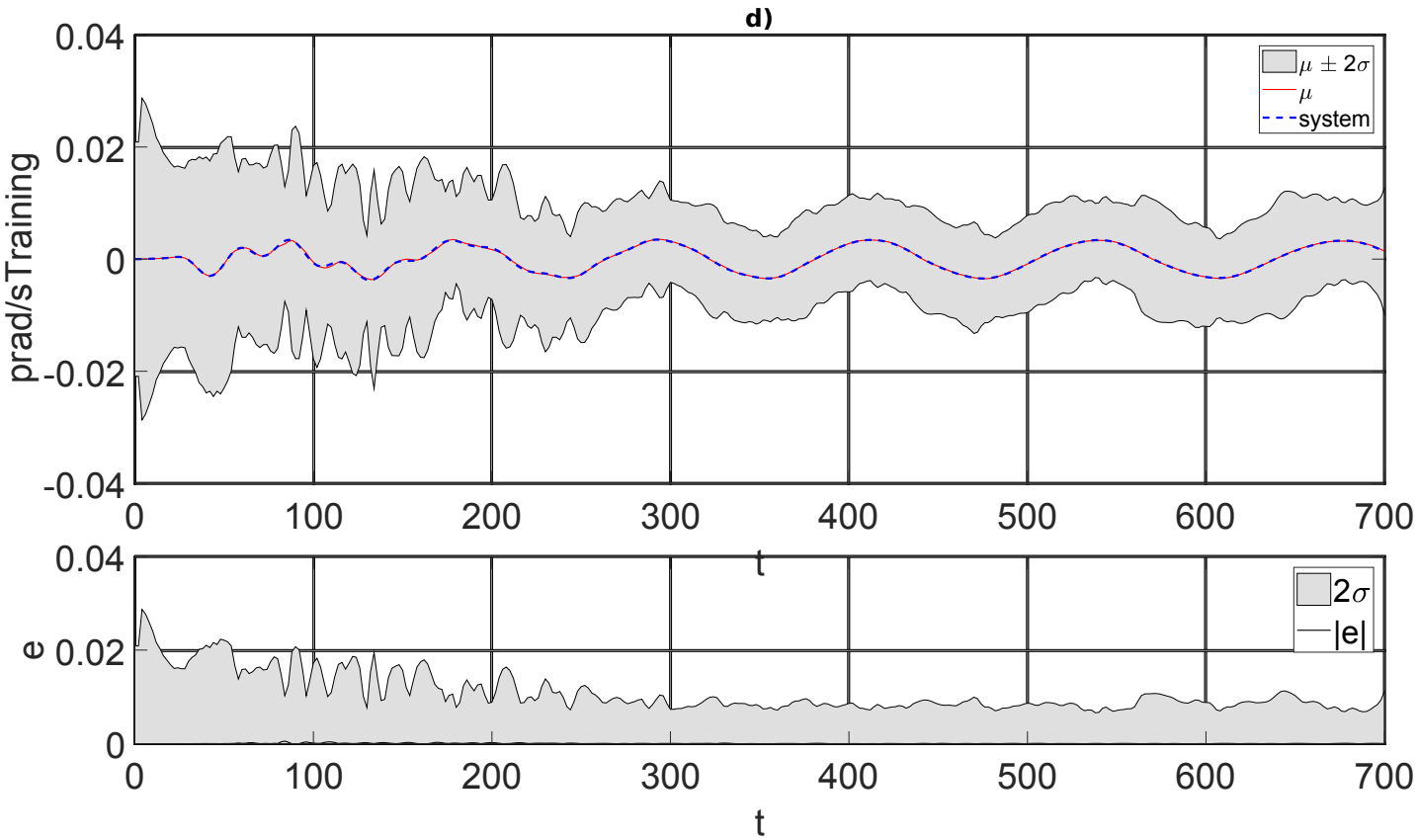
d)
0.04
0.02
0
-0.02
-0.04
prad/sTraining
0
100
200
300
400
500
600
700
t
$\mu \pm 2\sigma$
$\mu$
system
0.04
0.02
0
e
$2\sigma$
|e|
0
100
200
300
400
500
600
700
t

**Figure 7 a**

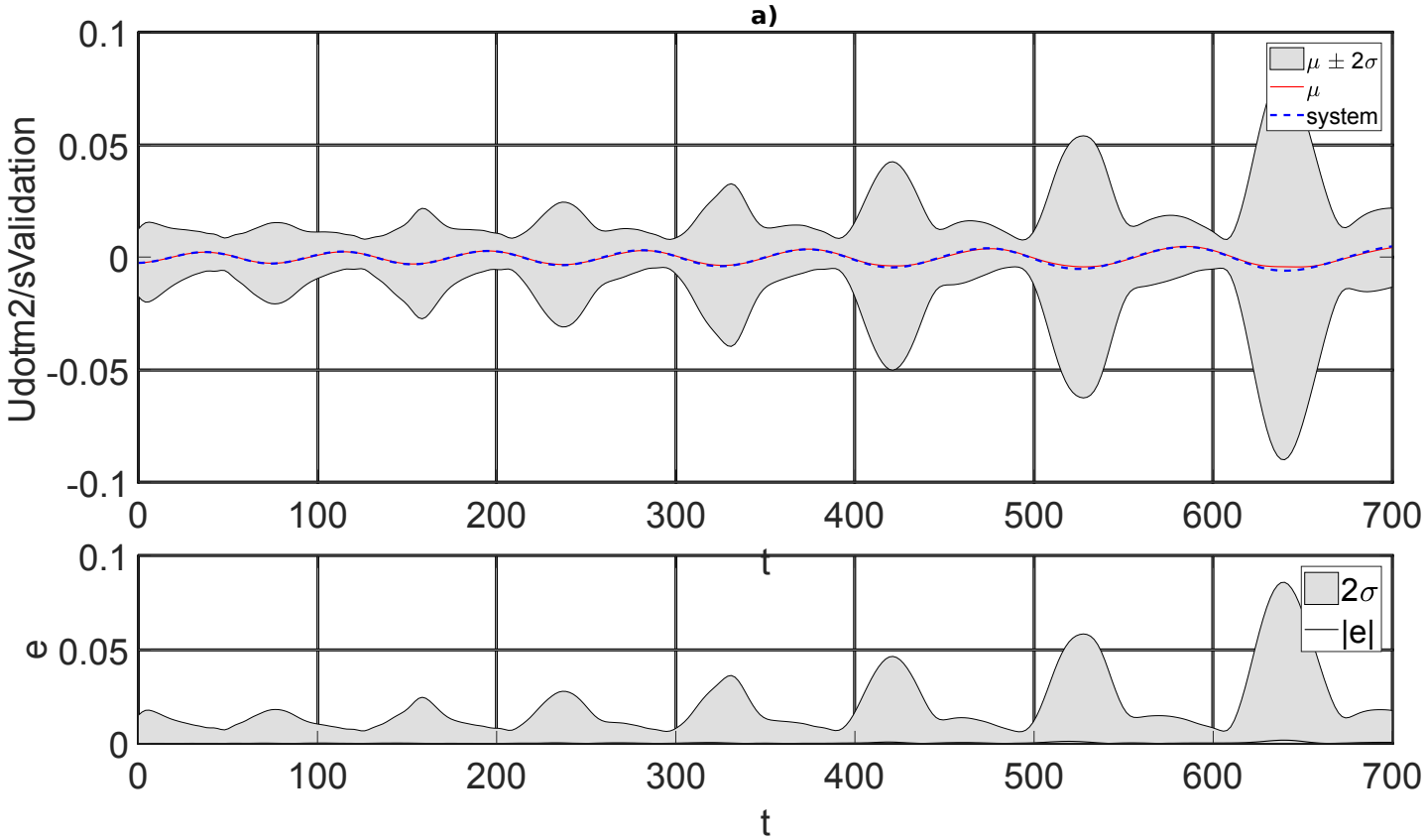
a)
0.1
0.05
0
-0.05
-0.1
Udotm2/sValidation
$\mu \pm 2\sigma$
$\mu$
system
0
100
200
300
400
500
600
700
t
0.1
0.05
0
e
$2\sigma$
|e|
0
100
200
300
400
500
600
700
t

**Figure 7 b**

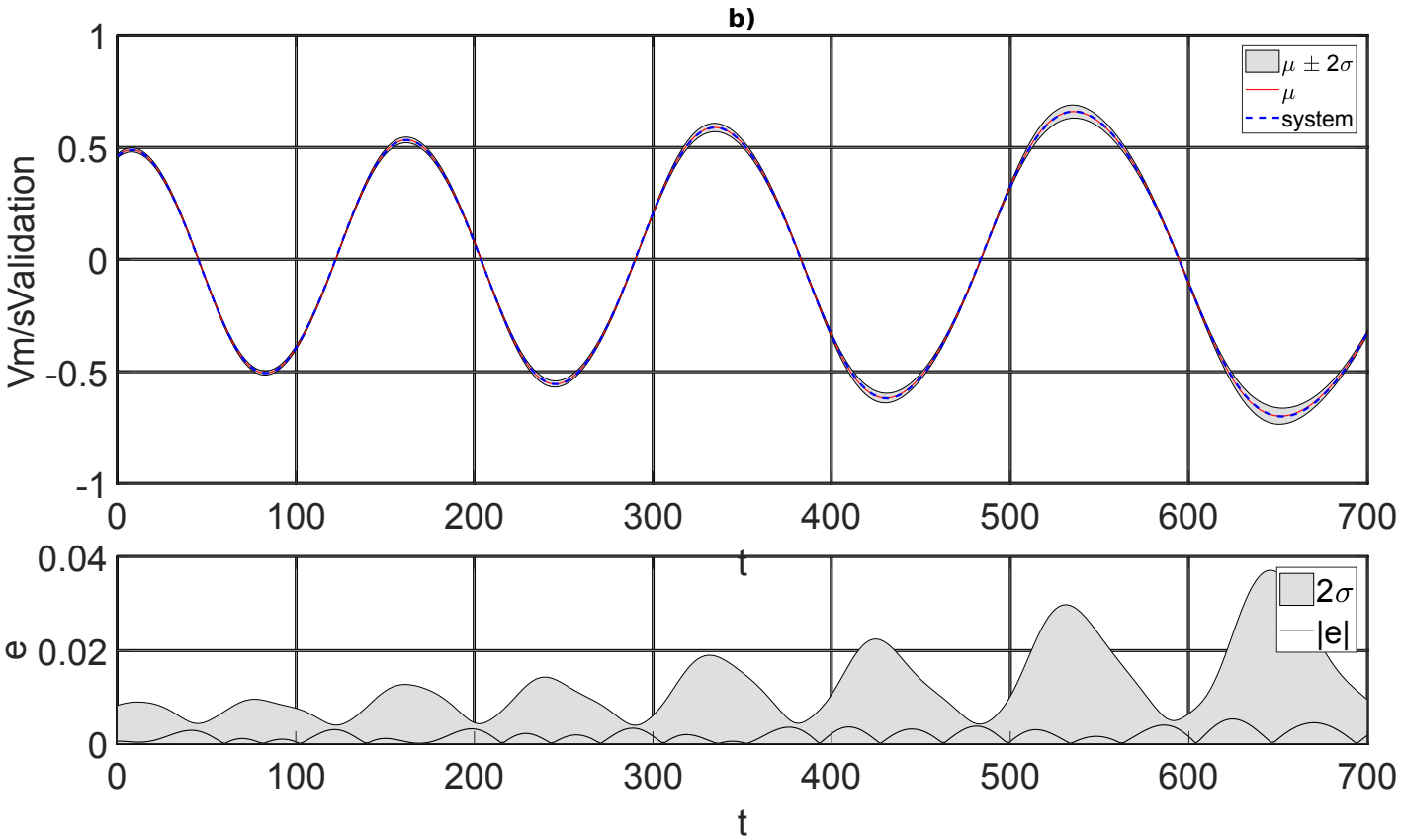
b)
Vm/sValidation
1
0.5
0
-0.5
-1
0
100
200
300
400
500
600
700
t
$\mu \pm 2\sigma$
$\mu$
system
e
0.04
0.02
0
$2\sigma$
|e|

**Figure 7 c**

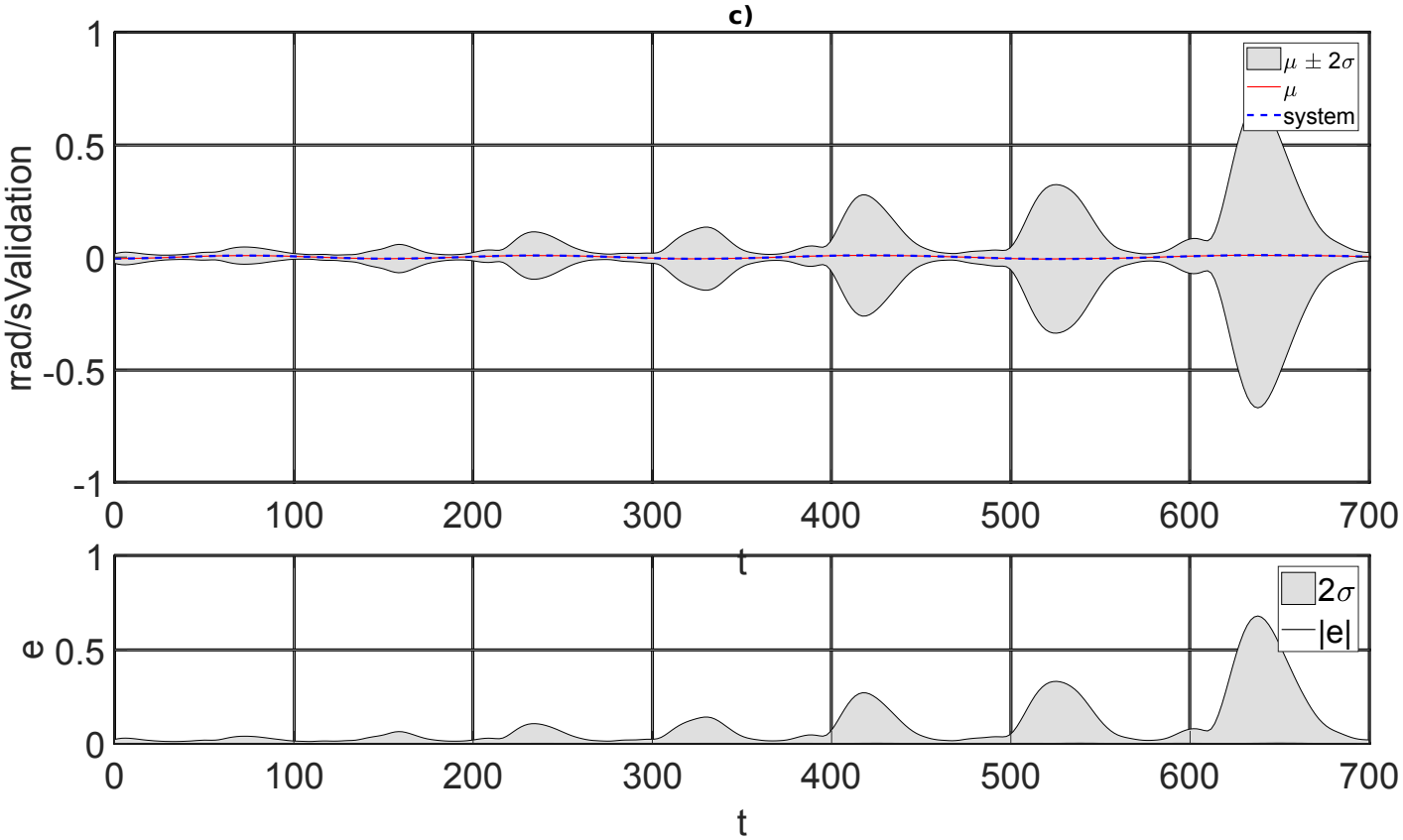
c)
rrad/sValidation
1
0.5
0
-0.5
-1
0
100
200
300
400
500
600
700
t
$\mu \pm 2\sigma$
$\mu$
system
e
1
0.5
0
0
100
200
300
400
500
600
700
t
$2\sigma$
|e|

**Figure 7 d**

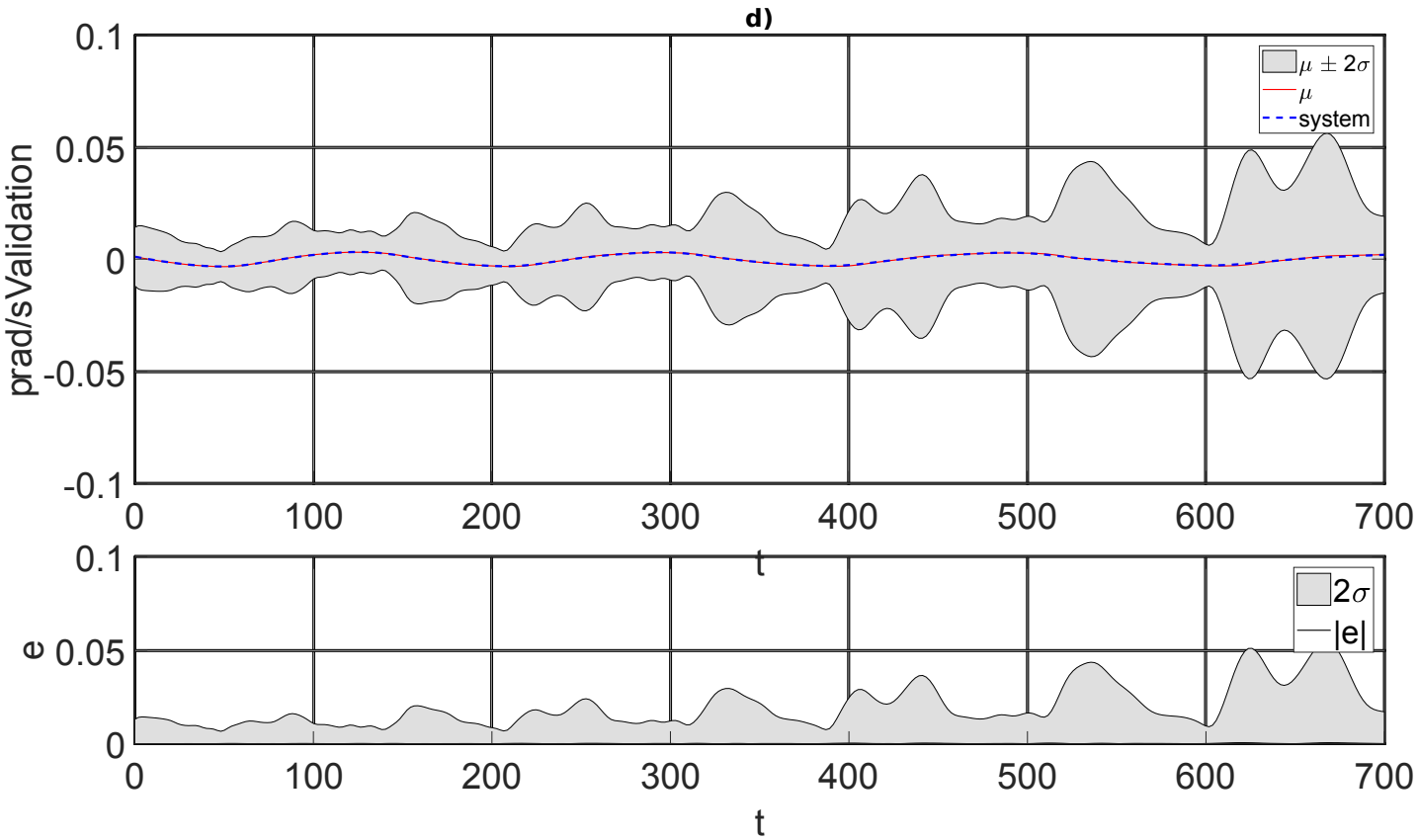
d)
0.1
0.05
0
-0.05
-0.1
prad/sValidation
$\mu \pm 2\sigma$
$\mu$
system
0
100
200
300
400
500
600
700
t
0.1
0.05
0
e
$2\sigma$
|e|
0
100
200
300
400
500
600
700
t

**Figure 8a**

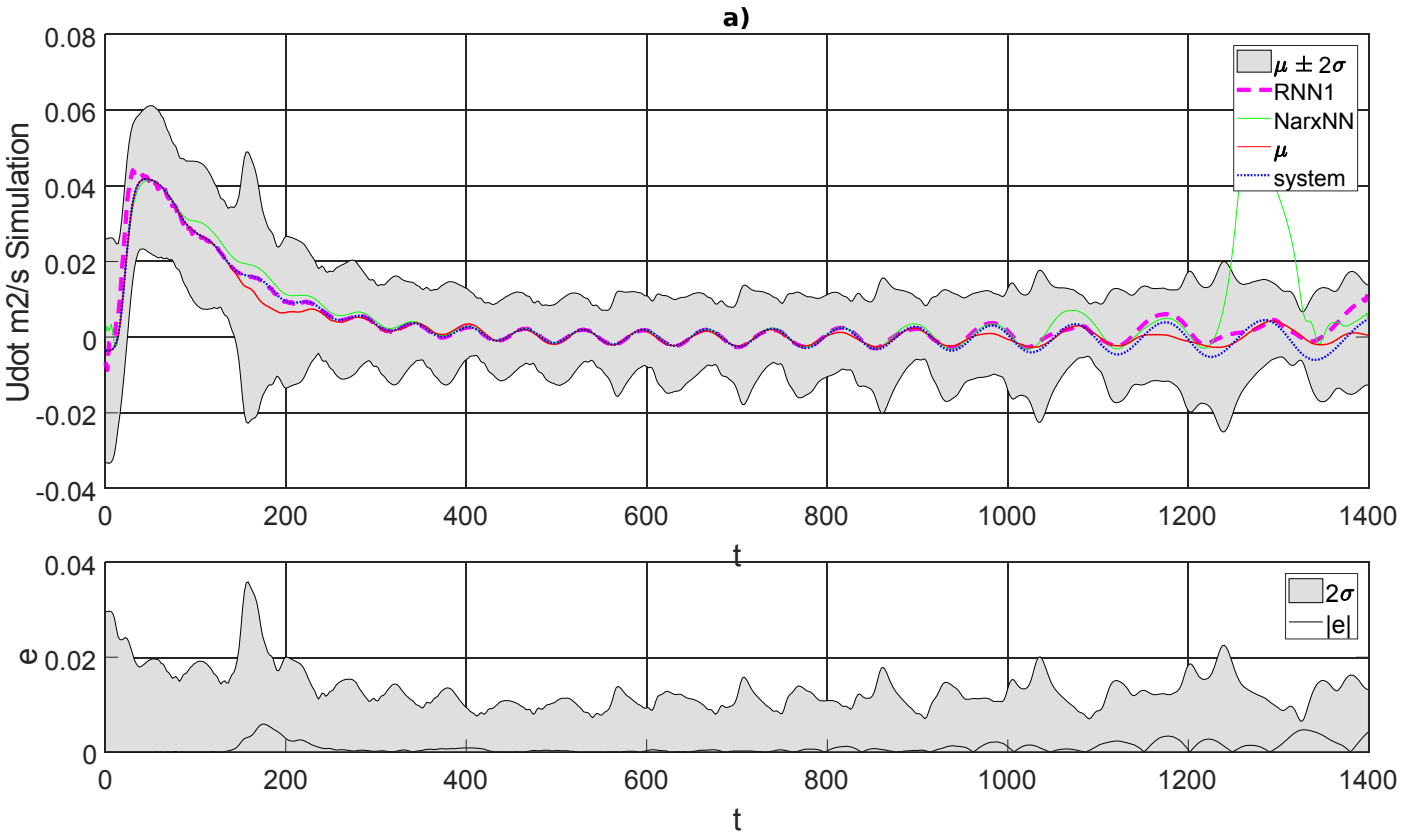
a)
Udot m2/s Simulation
0.08
0.06
0.04
0.02
0
-0.02
-0.04
0
200
400
600
800
1000
1200
1400
t
μ ± 2σ
RNN1
NarxNN
μ
system
e
0.04
0.02
0
2σ
|e|

**Figure 8b**

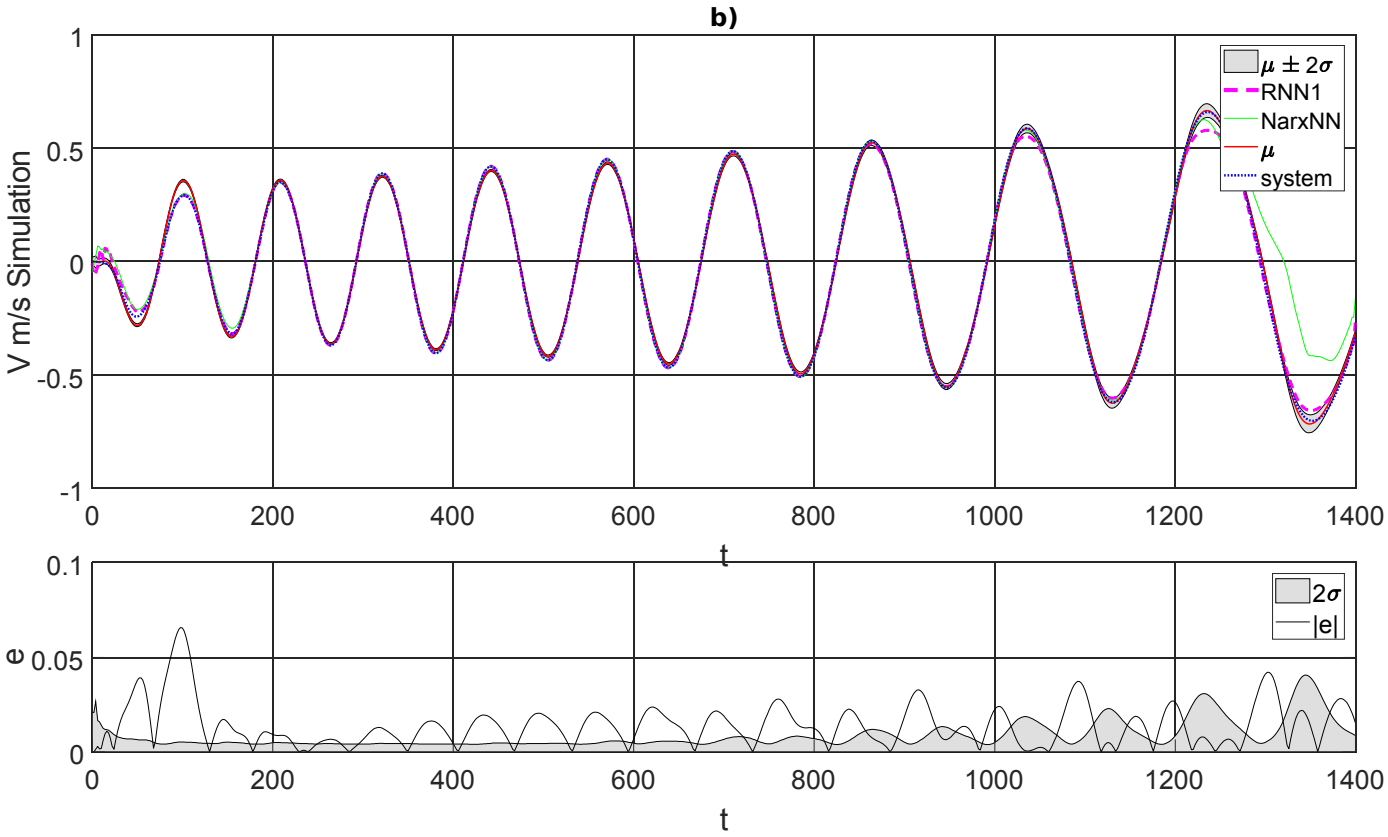

**Figure 8c**

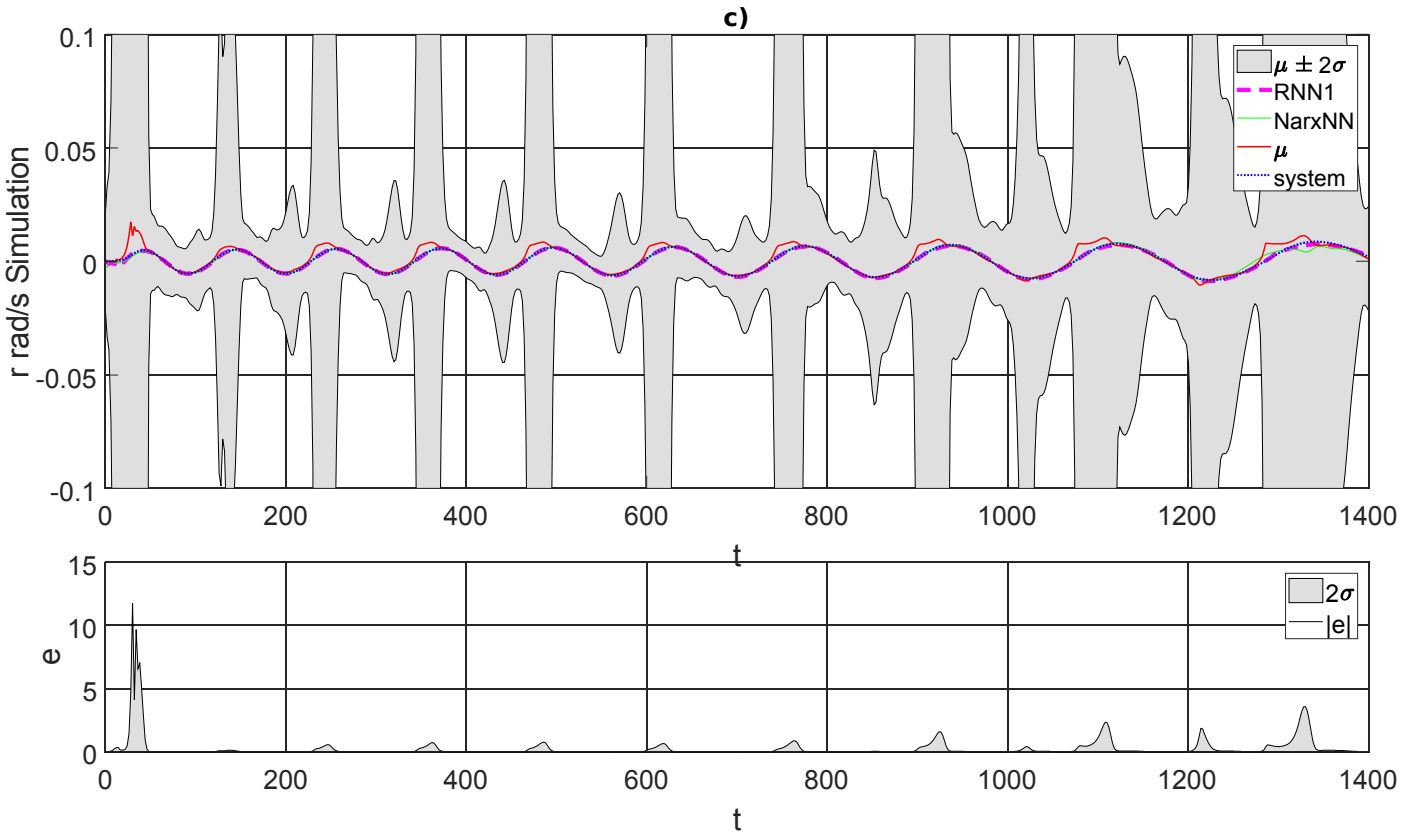
c)
r rad/s Simulation
0.1
0.05
0
-0.05
-0.1
0
200
400
600
800
1000
1200
1400
t
μ ± 2σ
RNN1
NarxNN
μ
system
e
15
10
5
0
2σ
|e|

**Figure 8d**

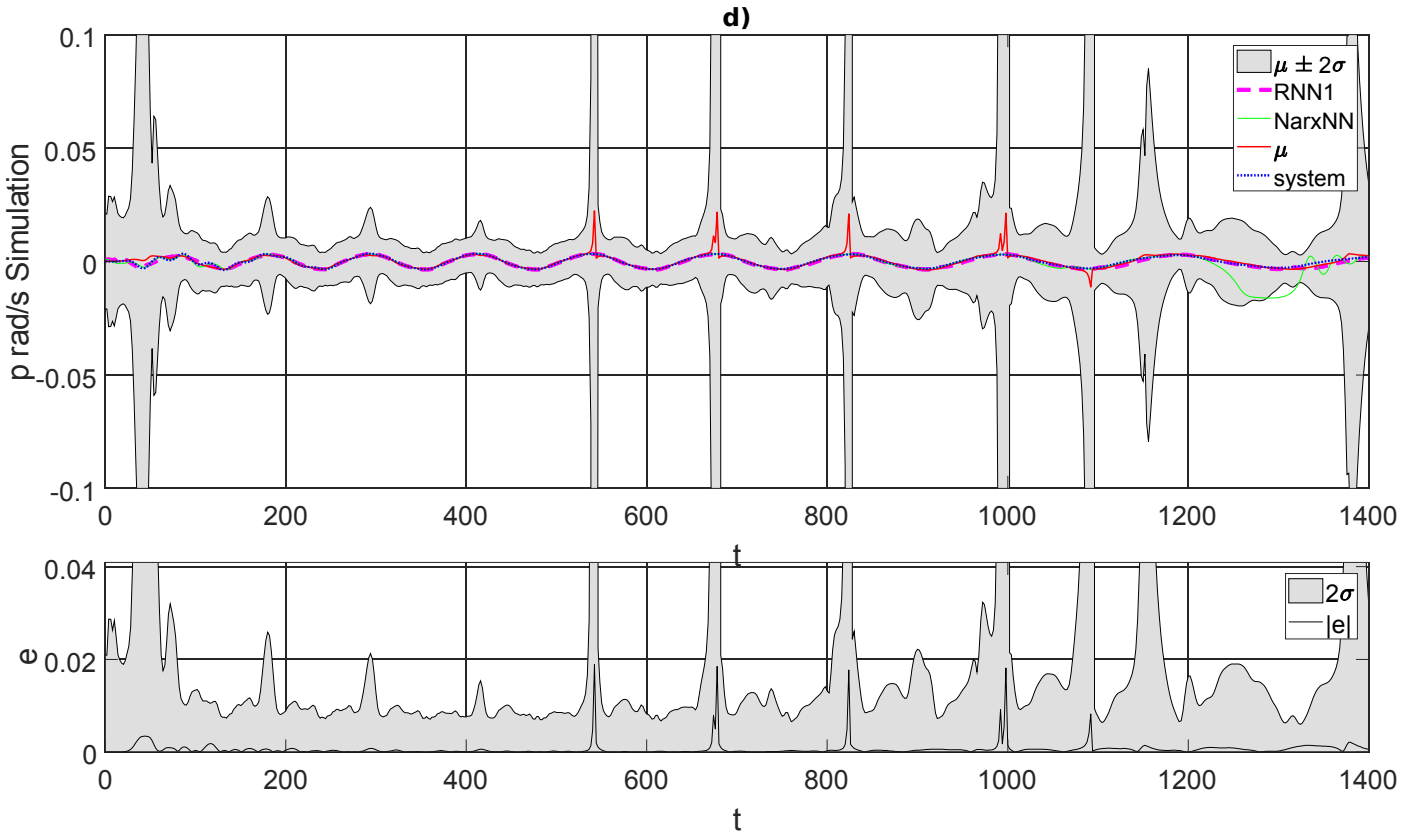
d)
p rad/s Simulation
0.1
0.05
0
-0.05
-0.1
0
200
400
600
800
1000
1200
1400
t
μ ± 2σ
RNN1
NarxNN
μ
system
e
0.04
0.02
0
2σ
|e|
t